Available online at www.sciencedirect.com
SCIENCE DIRECT®
Biochimica et Biophysica Acta 1663 (2004) 19–51
BIOCHIMICA ET BIOPHYSICA ACTA
BBA
www.bba-direct.com

Review

New insights into water–phospholipid model membrane interactions

Jeannine Milhaud*

Laboratoire de Physico-chimie Biomoléculaire et Cellulaire/Chimie et Spectroscopie Structurale Biomoléculaire (LPBC/CSSB), UMR CNRS 7033 (Box 138), Université Pierre et Marie Curie, 4 Place Jussieu 75252, Paris Cedex 05, France

Received 23 April 2003; received in revised form 22 January 2004; accepted 4 February 2004

Available online 13 March 2004

Abstract

Modulating the relative humidity (RH) of the ambient gas phase of a phospholipid/water sample for modifying the activity of phospholipid-sorbed water [humidity-controlled osmotic stress methods, J. Chem. Phys. 92 (1990) 4519 and J. Phys. Chem. 96 (1992) 446] has opened a new field of research of paramount importance. New types of phase transitions, occurring at specific values of this activity, have been then disclosed. Hence, it is become recognized that this activity, like the temperature *T*, is an intensive parameter of the thermodynamical state of these samples. This state can be therefore changed (phase transition) either, by modulating *T* at a given water activity (a given hydration level), or, by modulating the water activity, at a given *T*. The underlying mechanisms of these two types of transition differ, especially when they appear as disorderings of fatty chains. In lyotropic transitions, this disordering follows from two thermodynamical laws. First, acting on the activity (the chemical potential) of water external to a phospholipid/water sample, a transbilayer gradient of water chemical potential is created, leading to a transbilayer flux of water (Fick's law). Second, water molecules present within the hydrocarbon region of this phospholipid bilayer interact with phospholipid molecules through their chemical potential (Gibbs–Duhem relation): the conformational state of fatty chains (the thermodynamical state of the phospholipid molecules) changes. This process is slow, as revealed by osmotic stress time-resolved experiments. In thermal chain-melting transitions, the first rapid step is the disordering of fatty chains of a fraction of phospholipid molecules. It occurs a few degrees before the main transition temperature, T_m, during the pretransition and the sub-main transition. The second step, less rapid, is the redistribution of water molecules between the different parts of the sample, as revealed by T-jump time-resolved experiments. Finally, in lyotropic and thermal transitions, hydration and conformation are linked but the order of anteriority of their change, in each case, is probably not the same.

In this review, first, the interactions of phospholipid submolecular fragments and water molecules, in the interfacial and hydrocarbon regions of phospholipid/water multibilayer stacks, will be described. Second, the coupling of the conformational states of phospholipid and water molecules, during thermal and lyotropic transitions, will be demonstrated through examples.

Keywords: Phospholipid/water multibilayer; Interdependence of water and phospholipid chemical potential; Energetics of a phospholipid sample hydration; Transmembrane water transport; Properties of interfacial water; Humidity-controlled osmotic stress

1. Introduction

Water is the bathing medium of most biological assemblies. However, many of its properties are still poorly understood. Despite this poor understanding, it is becoming recognized that water molecules trapped in the infractuosities of the interface of biological assemblies play an essential role. As a matter of fact, owing to their small size, water molecules can occupy the smallest free-volumes within these assemblies (Sections 4.2 and 4.3) and, thereby, can induce important effects on their conformation through the interdependence of their chemical potential and that of biological assemblies (Section 2.7, [1,2]). As regards the

Abbreviations: DSC, differential scanning calorimetry; FT-IR, Fourier transform-infrared spectroscopy; NMR, nuclear magnetic resonance; LUV, large unilamellar vesicle; MLV, multilamellar vesicles; DLPC, dilauroylphosphatidylcholine; EPC, egg yolk phosphatidylcholine; DMPC, dimyristoylphsphatidylcholine; DPPC, dipalmitoylphosphatidylcholine; DODPC, dioctadecadienoylphosphatidylcholine; DOPC, dioleoylphosphatidylcholine; POPC, 1-pamitoyl-2-oleoylphosphatidylcholine; SDPC, 1-sterayol-2-docosahexaenoylphosphatidylcholine; DTDPC, bis-11, 13-tetradecadienoylphosphatidylcholine; DTDPE, bis-11, 13-tetradecadienoylphosphatidylcholine; POPE, 1-palmitoyl-2-oleoylphosphatidylcholine; DLPE, dilauroylphosphatidylethanolamine; DMPE, dimirystoylphosphatidylethanolamine; DOPE, dioleoylphosphatidylethanolamine; REES, red edge excitation shift; ITC, isothermal titration calorimetry

* Tel.: +33-1-44-27-42-34; fax: +33-01-44-27-75-60.
E-mail address: milhaud@ccr.jussieu.fr (J. Milhaud).

0005-2736/$ - see front matter © 2004 Elsevier B.V. All rights reserved.
doi:10.1016/j.bbamem.2004.02.003

phospholipid matrix of cell membranes, its interaction with bathing water depends on the location of the water molecules with respect to the phospholipid ones. Water molecules, if present as an external medium, govern the aggregation mode of phospholipid molecules, due to the hydrophobic effect by which their apolar parts (the fatty chains) are shielded from a contact with water for minimizing the overall free energy. The shape of resulting phospholipid aggregates depends on the interplay of different forces, such as the van der Waals attractive forces between fatty chains and the repulsive forces between the electric dipoles of the PCs and PEs polar heads, for instance. Water molecules, if located in spaces between headgroups, form intramolecular and intermolecular H-bonded cross-bridges between these headgroups (Section 3.4). Water molecules, if trapped in the interbilayer spacing of phospholipid/water multibilayers, mediate hydration forces (Section 3.1, [3]). Finally, water, added to dry phospholipid micelles in an apolar solvent, leads to water-in-oil microemulsions (reverse micelles, Section 3.6). In these microemulsions, phospholipid molecules are assembled as a monolayer at the interface between the water and the apolar solvent. In addition to these known effects, it is becoming evident that water molecules accommodated in the free-volumes of the hydrocarbon region (Section 4.3) act on the conformation of fatty chains (Section 5.3.2). This last point will be discussed below based on recent experimental results.

Till a few years ago, the control of the thermodynamical state of water was poor. Recently, the innovative method of humidity-controlled osmotic stress (Section 2.7) has enabled to adjust this state precisely. Several essential aspects of membrane–water interactions have thus become better understood, owing to several experimental methods presented in Section 2. Owing to new calorimetric methods, the energetics of the binding of water molecules to model membranes has been determined (Section 2.8, [4,5]). Owing to ^{2}H-NMR measurements, the motions of the phospholipid headgroups of labelled phospholipid/water multibilayers have been found to be governed by the activity of the interbilayer water (Section 3.5, [6,7]). Owing to vibrational spectroscopies and linear dichroism (using oriented phospholipid films), conformational changes of phospholipid submolecular fragments and interfacial water molecules have been found to be coupled (Section 5.3.1, Ref. [8] and references therein). In addition, simulation methods, which have known a recent huge development [9], have provided experimentally inaccessible information.

The goal of this review is commenting on these breakthroughs without eluding their thermodynamical sources essential to their recognition. The review of the relevant bibliography has ended with the year 2003. We will essentially discuss results obtained with the most studied phospholipids, i.e. electrically neutral phosphatidylcholines (PCs) and phosphatidylethanolamines (PEs) with symmetric saturated and monounsaturated fatty chains. We will concentrate on phospholipid/water multibilayers which are the most thermodynamically stable form of phospholipid lamellar phases.

2. Experimental methods of study

Methods used to extract information on the structure and the dynamics of phospholipid/water multibilayers resemble windows opened up to a moving panorama. During their aperture, the positions of atoms of phospholipid molecules and the exchanges between the different pools of sorbed water (Sections 3.2.2 and 5.2.2) are time-averaged. From then on, the spatial scale (microscopic or mesoscopic) in which the positions of atoms of phospholipid and water molecules are averaged depends on the time window of the observation method [10].

2.1. X-ray and neutron scattering

X-ray and neutron radiations can inform on the structural order of assemblies of phospholipid and water molecules.

The small-angle X-ray diffraction patterns consist of a series of sharp lines representing the successive orders of diffraction by the lattice formed by repetition of unit cells [11]. From their interval, the dimensions of these unit cells, like the lamellar repeat period for lamellar phases, ℓ, can be directly deduced. In addition, the profiles of these diffraction lines give access to the distribution of the electron density in the sample. In case of lamellar phases, this distribution exhibits two maxima, corresponding to the electron-dense phosphate headgroups, and a minimum corresponding to the center of these bilayers (Fig. 8b). The interval between the maxima provides, directly, the head–head separation in these bilayers and, indirectly, the thickness of their hydrophobic region after assessing the thickness of the hydrophilic region [12].

The wide-angle X-ray reflections correspond to the chain packing in a cross-section perpendicular to the normal to a phospholipid bilayer. They provide direct information on this packing.

A combination of X-ray and neutron diffraction data with computer-aided fitting has enabled to obtain the positions of the different phospholipid submolecular fragments along the normal to a phospholipid bilayer [13]. The resulting distributions of the probabilities of occupancy of these fragments along the bilayer normal reflect the *short-range fluctuations* responsible for the disorder within a unit cell of the lattice (Section 4.1). The *long-range fluctuations* in the relative positions of the different unit cells have been recently determined by Petrache et al. [14] and the relevant "liquid" crystallography method reviewed by Nagle and Tristram-Nagle [15].

2.2. NMR spectroscopy

In NMR experiments the energy levels of the spins of atom nuclei are governed by the interaction between a static

magnetic field and the electric field gradient (efg) of the chemical bond binding, for instance, a deuteron atom to another atom (the tensor V). ^{2}H-NMR spectra provide two types of information (for an example of spectrum, see Fig. 12). First, the interval between the two resonance lines, i.e. the quadrupolar splitting $\Delta\nu_Q$, informs us on the degree of order of the orientation of a D-containing fragment. This orientation can be defined with respect to a director axis, D (which is the bilayer normal in lamellar phases). The angle β between a C–D bond and D suffers thermal fluctuations which can be expressed in the form of an order parameter, S_{CD}, as:

$$S_{CD} = 1/2\langle 3\cos^2\beta - 1\rangle \quad (1)$$

where the brackets denote a time averaging. If D makes itself an angle θ with the static magnetic field, the expression of $\Delta\nu_Q$, as a function of S_{CD} and θ, is [16]:

$$\Delta\nu_Q = 3/2(e^2qQ/h)S_{CD}(3\cos^2\theta - 1). \quad (2)$$

At each θ value corresponds one $\Delta\nu_Q$ value. If the sample (in a lamellar phase, for instance) is not oriented, the spectrum is an average over all the molecular orientations (a powder-type spectrum). The extraction of each $\Delta\nu_Q$ value corresponding to each θ value requires either a deconvolution of the spectrum (DePacking procedure) or a macroscopic orientation of the sample. Knowing $\Delta\nu_Q = f(\theta)$, S_{CD} can be calculated from Eq. (2).

The time window of ^{2}H-NMR experiments is about 10^{-5} s: during this time interval, the molecular motions are averaged. Nevertheless, information about these motions is accessible by measurements of the relaxation times following sequences of pulses of magnetic field, resulting in an echo signal. From the attenuation of this echo due to thermal motions, one can deduce the dynamics of the orientation of the D-containing fragment corresponding to different correlation times.

2.2.1. Correlation times assignable to different types of motions

Let us consider the time-dependent position of a D atom, defined by a structural parameter X. At the instants t and $t+\tau$, the values of X barely differ if τ is small: $X(t+\tau)$ is called "correlated" with X(t). According to the magnitude of τ, the time-averaged product, $\langle X(0)\times X(\tau)\rangle$, takes different values. For $\tau = 0$, we have:

$$\langle X(0)\times X(\tau)\rangle = \langle X(0)^2\rangle. \quad (3)$$

For τ values large with respect to the characteristic period of the fluctuations of X, the correlation vanishes and we have:

$$\lim(\tau\to\infty)\langle X(0)\times X(\tau)\rangle = \langle X(0)\rangle\times\langle X(\tau)\rangle = \langle X\rangle^2. \quad (4)$$

The decrease of $\langle X(0)\times X(\tau)\rangle$ from $\langle X^2\rangle$ up to $\langle X\rangle^2$ can be described by the exponential $\exp(-\tau/\tau_c)$ where τ_c is the correlation time of the parameter X.

The relaxation times T_1 and T_2 correspond to two types of echo attenuation. The spin–spin (transverse) relaxation time, T_2, characterizes slow thermal motions ($\tau_c \sim 10^{-6}$ s) whereas the spin-lattice (longitudinal) relaxation time, T_1, reflects the energy exchanges between the spin system and the lattice. It is related to the corresponding correlation time, τ_c, as [17]:

$$1/T_1 = 3/8(e^2qQ/h)^2(1 - S_{CD}^2)\tau_c. \quad (5)$$

T_1 is relevant to fast motions (10^{-7} s $\le \tau_c \le 10^{-10}$ s) such as the rotation of molecules as a whole ($10^{-10} < \tau_c < 10^{-9}$ s) and their lateral diffusion ($\tau_c \sim 5\times10^{-8}$ s). Let us note that the motions of methylene groups within the phospholipid fatty chains are much faster ($\tau_c \sim 5$–20×10^{-12} s).

2.3. FT-IR spectroscopy

The absorbance of an IR radiation in a region of the FT-IR spectra, A, is function of the amplitude of the electric field of the incident radiation, $|E|$, and of the oscillating transition moment, $|\partial\mu/\partial Q|$ (the variation of the electric dipole along the coordinate Q):

$$A \propto |E.\partial\mu/\partial Q|^2 = |E|^2\times|\partial\mu/\partial Q|^2\cos^2\Gamma. \quad (6)$$

In Eq. (6), Γ is the angle between the E and $\partial\mu/\partial Q$ vectors. Through this angle, the magnitude of the absorbance informs us about the orientation of $\partial\mu/\partial Q$, i.e. the orientation of the corresponding chemical bond, on the condition that the sample is macroscopically oriented and the radiation linearly polarized. In Fig. 1 [18] is schematized a polarized attenuated total reflection (ATR) experiment in which the phospholipid film is spread on a crystal (of germanium or ZnSe) and the polarized IR beam totally reflected. The resulting evanescent wave is absorbed by the phospholipid film. This ATR method has two advantages: (i) the orientation of the film enables linear dichroism measurements to be performed; (ii) the absorption of the solvent (water) is greatly attenuated preventing an overlap of the water and phospholipid CH_2 FT-IR bands. The dichroic ratio is defined as [18]:

$$R = A_{//}/A_\perp = (E_{//}\times\partial\mu/\partial Q)^2/(E_\perp\times\partial\mu/\partial Q)^2 \quad (7)$$

where $A_{//}$ and $A_\perp$ are the absorbances corresponding to polarization planes parallel and perpendicular, respectively, to the Y-axis (components of the electric field equal, respectively, to $E_{//}$ and $E_\perp$). If the orientation of the chemical bond corresponding to the transition moment of interest makes an angle Γ with the bilayer normal (the Z-symmetry-axis in Fig. 1), the order parameter, S_{IR},

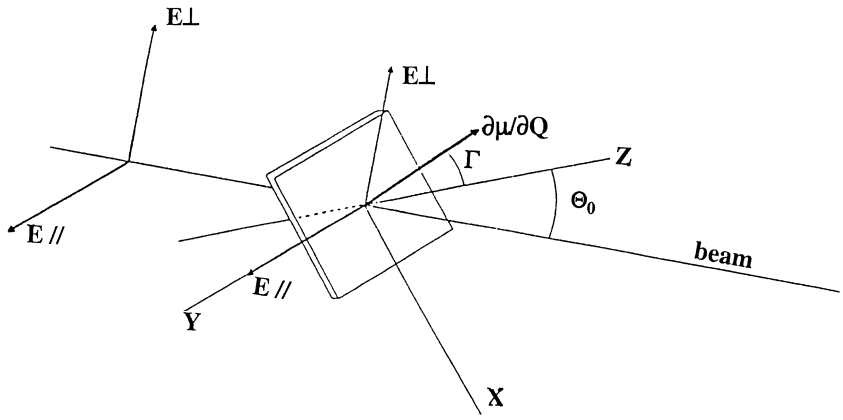

Fig. 1. Geometry of the different orientations axises in an experiment of ATR FT-IR linear dichroism, reproduced from Ref. [18] with permission. An orthogonal system of axises, *X*, *Y* and *Z*, is linked to a phospholipid/water multibilayer sample spread on a crystal, with the bilayer normal confounded with the *Z*-axis. *E*⊥ and *E*// represent the directions of the two polarization planes of the incident IR radiation, the latter being parallel to *Y*. The orientation of the oscillating transition moment, $\partial\mu/\partial Q$, is shown to make an angle Γ with the bilayer normal.

corresponding to the statistical average of its orientation, is defined as:

$$S_{IR} = 1/2\langle 3\cos^2\Gamma - 1\rangle. \quad (8)$$

If θ_0 is equal to 45° (Fig. 1), the ratio of the refractive indices of the phospholipid film and the crystal equal to 0.6 (ZnSe crystal), and the phospholipid film thick, the dichroic ratio is equal to [19]:

$$R = (2 + 2.55S_{IR})/1 - S_{IR}. \quad (9)$$

Hence, S_{IR} can be calculated knowing *R*.

2.3.1. Informations provided by IR bands on the state of interfacial water

The broad IR ν_{13}(OH) band, centered at 3400 cm^{-1}, corresponds to several coupled OH vibrational modes: the fundamental symmetrical (ν_1) and antisymmetrical (ν_3) stretching, and the second overtone of the bending (ν_2) vibrational modes. These different modes can be uncoupled by using 1:9 mol/mol H_2O/D_2O mixtures (Section 5.3.1.1).

Besides, FT-IR spectroscopy is especially suitable for identifying H-bonds between interfacial water molecules and phospholipid headgroups. Generally speaking, the formation of a H-bonded complex between two atoms A and B, A–H...B, leads to a weakening of the A–H bond and, thereby, a downshift of the frequency of the A–H stretching vibration by a few tens of cm^{-1}. The width in frequency of the ν_{13}(OH) band reflects the distribution in strength of the H-bonds between phospholipid and interfacial water molecules.

2.4. Fluorescence spectroscopy

In fluorescence experiments, a fluorescent probe absorbs a photon and emits another one from its lowest excited state, after a fast nonradiative relaxation. This process corresponds to a time window of about 10^{-9} s. The water molecules present in the environment of such probes are able to modify, at one and the same time, their steady and time-resolved emission spectra enabling the hydration level [20] as well as the dynamics of this hydration [21] to be probed.

The first approach (wavelength-selective fluorescence or REES effect, [20]) is based on the red-edge effect shifting fluorescence emission spectra. It rests on the similarity between the lifetime of the excited state of a fluorophore ($\sim 10^{-9}$ s) and the delay required for the reorientation of the water dipoles surrounding it (if present) due to the electric field created by its excitation. Its observation requires that the fluorophore has differently relaxed states and that its excitation increases its dipole moment. From then on, if this excitation arises from the red-edge of its excitation spectrum, it will selectively excite the molecules surrounded by water dipoles oriented like in a relaxed state. The resulting emission spectrum is shifted with respect to that resulting from an excitation at the maximum of the excitation spectrum: this is the REES effect.

The second approach (solvation dynamics [21]) is based on the time-dependent shift of the fluorescence emission spectrum of a fluorophore excited by light pulses (Stokes shift due to the reorientation of surrounding water dipoles), during the delay for its emission. The resulting time-resolved emission spectra enable to assess the dynamics of reorientation of these water dipoles. This dynamics has provided information on the delay for the exchange of phospholipid-H-bonded interfacial water molecules with neighbouring molecules, able to replace them after their release (Section 3.6).

When the fluorescence absorption spectrum of a molecule (an acceptor) overlaps the fluorescence emission spectrum of another neighbouring molecule (a donor), an energy transfer from the excited donor to the acceptor can result, without the appearance of a photon: this is a

fluorescence resonance energy transfer (FRET). The rate of this transfer depends on the extent of the spectral overlap and of the distance between the donor and acceptor molecules [22].

2.5. Calorimetric methods

Two types of calorimetric methods are currently used to obtain information on the energetics of the thermodynamical transitions experienced by phospholipid/water multibilayers [23].

In *differential* scanning calorimeters, two cells containing respectively the phospholipid sample and the buffer are heated at the same programmed rate. If a thermally induced phase transition occurs in the sample, a disequilibrium in temperature between the two cells occurs due to the additional heat capacity of the sample, c_p, at the transition temperature. This disequilibrium should be cancelled by an additional electric power which informs us on the enthalpy of the phase transition, ΔH, through the relation:

$$\Delta H = \int c_p \mathrm{d}T. \tag{10}$$

In Eq. (10), the integration is made in the temperature range of this transition.

In *titration* calorimetry, one of two reactants (like water and phospholipid in a phospholipid/water sample) is stepwise added in a reaction cell, at fixed temperature. The heat evolved at each step informs us on the partial enthalpy (Δh_{hyd}, Section 2.8) at each stage of the reaction. In case of a phospholipid hydration, an abrupt change of Δh_{hyd} during the hydration process signals a lyotropically induced transition of this phospholipid (Section 5.3.1.2, Fig. 20).

2.6. Dielectric spectroscopy

Dielectric spectroscopy investigates the dynamics of electric dipoles, like those of PC and PE polar heads, and interfacial molecules bound to them, in alternating electric fields. The response of these composite dielectrics is reflected by their complex permittivity, $\varepsilon(\nu) = \varepsilon'(\nu) - i\varepsilon''(\nu)$, where the functions $\varepsilon'(\nu)$ and $\varepsilon''(\nu)$ represent the dielectric spectra [24]. The frequencies $\nu = (2\pi\tau)^{-1}$ at which $\varepsilon''(\nu)$ is maximum define the relaxation times. For the phospholipid polar head dipoles, these maxima take place around 10^6 Hz whereas, for associated water dipoles, they occur around 10^{10} Hz.

2.7. New humidity-controlled osmotic stress method

Generally speaking, within phospholipid/water multibilayer samples, internal water (water in the interbilayer spaces, schematized in Fig. 2 by the compartment II) should be distinguished from external water (the hydration source, schematized in Fig. 2 by the compartment I). When these two types of water molecules have different chemical potentials (different activities a_w^I and a_w^{II}), the system is not at equilibrium. This disequilibrium generates a flux of water across the peripheral phospholipid bilayer (schematized by dashes in Fig. 2). This flux, $J(z)$, flows in the direction of the negative gradient of the water chemical potential (Fick's law, [25]). It can be expressed as:

$$J(z) = -[C(z) \times D(z)/RT] \times \mathrm{d}\mu(z)/\mathrm{d}z \tag{11}$$

where $C(z)$ and $D(z)$ denote, respectively, the concentration and the diffusion coefficient of water at the position z along the bilayer normal. This transport phenomenon can be more generally written, in the formalism of the nonequilibrium thermodynamics, as a relationship between a flux and a "conjugate" force through a phenomenological coefficient, as schematized in Fig. 3 [25]. When the "conjugate" force is a difference of osmotic pressure between the hydration source and the interbilayer spaces (compartments I and II in Fig. 2), it is spoken of an osmotic stress of the sample.

The osmotic stress method consists in modulating the Gibbs free energy of a phospholipid/water sample by modifying the osmotic pressure of the hydration source. If n_L and n_w represent the number of phospholipid and associated water moles in one monolayer of phospholipid bilayer, and $\Delta\mu_L$ and $\Delta\mu_w^{II}$ their respective chemical potentials, the Gibbs free energy of this monolayer, per mole of phospholipid, at given temperature, T, and pressure, p, is:

$$G(T,p) = \Delta\mu_L + (n_w/n_L)\Delta\mu_w^{II} = \Delta\mu_L + R_w\Delta\mu_w^{II} \tag{12}$$

where R_w denotes the water-to-phospholipid molar ratio. As apparent from Eq. (12), the derivative of G with respect to R_w is the chemical potential of internal water:

$$(\partial G/\partial R_w)_{T,p} = \Delta\mu_w^{II}. \tag{13}$$

In Eqs. (12) and (13), $\Delta\mu_w^{II}$ and $\Delta\mu_L$ are referred to reference states represented by the compartment 0 in Fig. 2. These reference states are, for water, the pure free water ($a_w^0 = 1$, $\mu_w^o = 0$) and, for the phospholipid, the fully hydrated state in which the amount of internal water is large enough so that its activity is equal to that of free water. As a matter of fact, when the phospholipid is not fully hydrated, the activity of internal water is lower than that of free water. In fact, water molecules trapped in the interbilayer spaces of a phospholipid/water multibilayer are composed of numerous populations, which have different activities depending on their distance from the interface (Section 3.2.1). As a first approximation, they can be represented by a single space-averaged activity $a_w^{II} < 1$. If an osmolyte is introduced in the hydration source, leading to an osmotic pressure π_{osm}, the chemical potential of the water molecules of this source, $\Delta\mu_w^I$, is related to π_{osm} by:

$$\Delta\mu_w^I = RT\ln a_w^I = -v_w\pi_{osm} \tag{14}$$

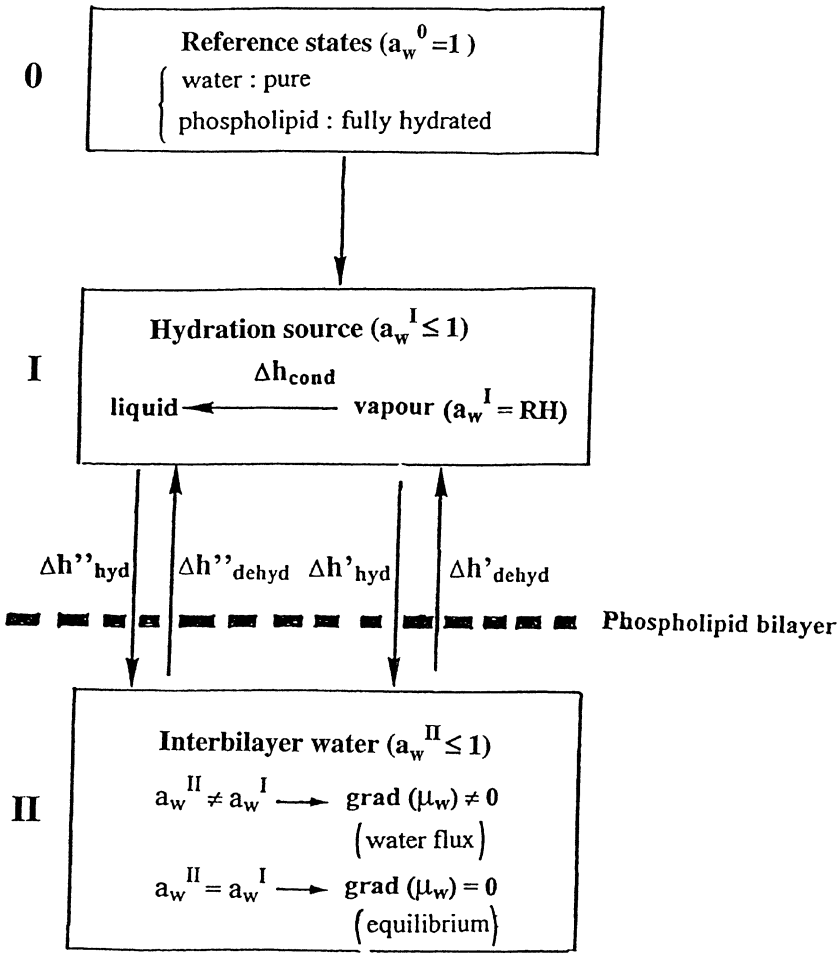

Fig. 2. Scheme of the different steps of hydration/dehydration of the peripheral bilayer of a phospholipid/water multibilayer sample. The compartments 0, I and II schematize respectively the reference states for phospholipid and water (activity equal to a_w^0), the thermodynamical state of water (liquid or vapour) in the hydration source (activity equal to a_w^I), and the thermodynamical state of the interbilayer water in the hydrated sample (activity equal to a_w^{II}). This peripheral phospholipid bilayer is schematized by dashes. The variations of the molar enthalpy during the transfer of 1 mol of water from the hydration source (I) to the sample (II) ($\Delta h'_{hyd}$ (vapour) or $\Delta h''_{hyd}$ (liquid)), or the inverse ($\Delta h'_{dehyd}$ (vapour) or $\Delta h''_{dehyd}$ (liquid)), are indicated by arrows. When no equilibrium exists between the states of water in I and II, a gradient of the water chemical potential across the peripheral phospholipid bilayer results, generating a flux of water across this bilayer (Fig. 3, Section 2.7, Eq. (11)).

where v_w is the molar volume of water. Under equilibrium conditions between compartments I and II (Fig. 2):

$$d(\Delta\mu_w^{II}) = d(\Delta\mu_w^{I}) = -v_w d\pi_{osm}. \quad (15)$$

Now, in the two-component phospholipid/water samples the chemical potentials of water and phospholipid components are interdependent, owing to the Gibbs–Duhem relation [25] which writes, at constant T and p, as:

$$d(\Delta\mu_L) + (n_w/n_L)d(\Delta\mu_w^{II}) = 0. \quad (16)$$

In the new humidity titration methods, initiated by Smith et al. [26] and recently developed by Binder et al. [4] and Markova et al. [5], *the hydration source is the water vapour*, the activity of which, a_w^I, is equal, by definition, to the ratio of the partial pressure of water vapour by the saturation pressure at the same temperature, i.e. the relative humidity of the gas phase, RH:

$$a_w^I = (p_w/p_{sat})^I = RH = \exp(\Delta\mu_w^I/RT). \quad (17)$$

Although in this case no osmolyte is present in the hydration source, this method is related to the osmotic stress method and called humidity-controlled osmotic stress. It has opened, owing to its simplicity, an attractive new field of research. Indeed, it permits to control the state of water in the hydration source and, consequently, the state of water in a phospholipid/water sample, better than a regulation of the osmotic stress by adding solutes to external water.

2.8. New calorimetric methods for measuring the energetics of the hydration of phospholipid model membranes

The energetics of the hydration of a phospholipid sample has been determined owing to new calorimetric methods. As

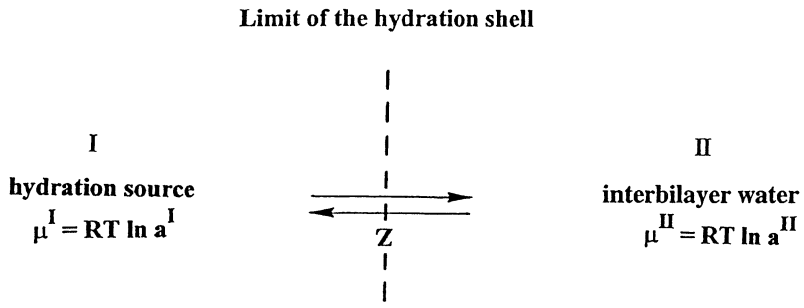

The water flux from I to II is associated to a "conjugate" force according to the relation:

Flux = phenomenological coefficient x driving force

hydraulic conductivity x reflection coefficient	**$\Delta\pi$ (difference of osmotic pressure)**
rate by force unit x concentration	**- dμ/dz (chemical potential gradient)**

Fig. 3. Scheme showing the exchange of water molecules between a hydration source (I) and the interbilayer spacing of a phospholipid/water multibilayer (II). The expression, in the formalism of the nonequilibrium thermodynamics [25], of the flux of water from I to II, as a function of the "conjugate" force, is given for two types of conjugate forces.

a matter of fact, this energetics is defined by the three interdependent following state functions which depend on the activity of the sorbed water:

$$\Delta G_{hyd}(a_w^{II}) = \Delta H_{hyd}(a_w^{II}) - T\Delta S_{hyd}(a_w^{II}). \quad (18)$$

In Eq. (18), ΔH_{hyd} and $T\Delta S_{hyd}$ are the enthalpic and entropic terms of the variation of the Gibbs free energy, ΔG_{hyd}.

In a first method [4], ΔG_{hyd} has been calculated by decomposing, for instance, a dehydration process into a series of elementary steps at the end of which the sample and the hydration source are in equilibrium ($a_w^{II} = a_w^I$ in Fig. 2). For each decrement of R_w, d(R_w), the small variation of ΔG_{dehyd} is:

$$\begin{aligned} d(\Delta G_{dehyd}) &= \Delta\mu_w^{II} \times d(R_w) = \Delta\mu_w^I \times d(R_w) \\ &= RT \ln a_w^I \times d(R_w). \end{aligned} \quad (19)$$

The global ΔG_{dehyd}, corresponding to a dehydration from the fully hydrated state to a state with a water activity equal to a, is obtained by integration of Eq. (19):

$$\begin{aligned} \Delta G_{dehyd}(T,a) &= \int_1^a \Delta\mu_w^{II}(a) \times [dR_w/da] \times da^I \\ &= RT \int_1^a \ln a^I \times R'_w \times da^I. \end{aligned} \quad (20)$$

Its calculation requires to know the function $R_w = f(a_w)$ at the temperature T, called a sorption isotherm.

Sorption isotherms have been generally assessed by gravimetry through equilibria between the phospholipid/water sample and a hydration source in which water molecules have different activities (cf. for instance Refs. [4,27]). However, in a second method, using an especially double-twin calorimeter, Markova et al. [28] have simultaneously determined the amount of water sorbed by a phospholipid and the corresponding enthalpy of hydration, ΔH_{hyd}. This calorimeter consists in two chambers (vaporization and sorption ones) containing, respectively, liquid water and the phospholipid sample, connected by a tube. The flow of vapour water from the vaporization chamber to the sorption one is controlled by the enthalpy of water vaporization and the diffusion through the connecting tube. Hence, on condition that the water flow remains constant (steady state in the connecting tube), both the sorption of water by the phospholipid and the corresponding partial enthalpy of hydration, $\Delta h'_{hyd}$, can be simultaneously measured *at a constant water activity* [5]. If the hydration is accompanied by a phase transition, it appears a plateau on the plot of ΔH_{hyd} versus R_w. The features of the sorption isotherms of phospholipids depend on the nature of their polar head and the degree of saturation of their fatty chains. The PC heads sorb more water than PE ones and the unsaturated phospholipids more water than the saturated ones. The R_w values at full hydration of PC and PE multibilayers, in various thermodynamical states, have been reviewed [29].

Finally, as a third method, Binder et al. [4], using a humidity titration calorimeter (Section 2.5), have independently determined ΔH_{hyd} from the heat exchanged between a phospholipid sample of known mass and a gas with controlled RH, circulating above it. The exchanged heat, corresponding to an infinitesimal sorption of *water vapor*,

$\Delta h'_{hyd}(a_w^I)$, is transformed into that corresponding to a sorption of *liquid water*, $\Delta h''_{hyd}$, through the relation:

$$\Delta h''_{hyd} = \Delta h'_{hyd} - \Delta h_{cond} = -\Delta h''_{dehyd} \quad (21)$$

where Δh_{cond} is the known molar heat of water condensation (-44.6 kJ/mol, at 25 °C). The cumulated variations of enthalpy accompanying a stepwise dehydration of a phospholipid sample from the fully hydrated ($a_w^{II}=1$) to a less hydrated ($a_w^{II}<1$) state is obtained by integration:

$$\Delta H''_{dehyd} = \int_1^{a_w} \Delta h''_{dehyd} \times (\partial R_w / \partial a_w^I) da_w^I. \quad (22)$$

The values of ΔG_{dehyd}, ΔH_{dehyd} and $-T\Delta S_{dehyd}$ (obtained by difference through Eq. (18)) during a dehydration of POPC/water multibilayers, at 25 °C, are represented in Fig. 4 [4]. The Gibbs free energy of dehydration is positive and significant only for $R_w<5$: the dehydration is not a spontaneous phenomenon. In this R_w range, ΔH_{dehyd} is negative (exothermic process) and decreases in absolute value when increasing R_w (vanishing for $R_w>5$). As to $-T\Delta S_{dehyd}$, it is positive (entropically unfavorable process), superior to ΔH_{dehyd}, and vanishes for $R_w>5$. In contrast, a *phospholipid hydration is a spontaneous phenomenon* where both the enthalpy and entropy variations are positive for $R_w<5$. The smaller the amount of sorbed water, the stronger is its interaction with phospholipid headgroups. Similar results have been obtained with Markova et al.'s [5] double-twin calorimeter.

The hydration-induced favorable gain in entropy has been assigned to motions of reorientation and protrusion of headgroups. As a matter of fact, the water accessible surface area (ASA) of fluid DPPC bilayers has been found by simulations [30] twice larger than the area projected perpendicularly to the bilayer normal, mainly because of the protrusion of the trimethylammonium headgroup.

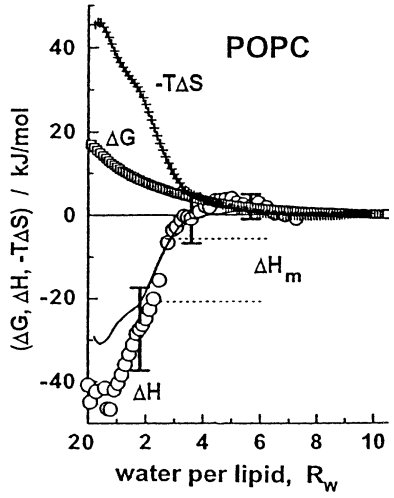

Fig. 4. Variations as a function of the water-to-phospholipid molar ratio, R_w, of the three state functions (ΔH, ΔG and $-T\Delta S$) defining the energetics of the dehydration of POPC multibilayers at 25 °C (reproduced from Binder et al. [4] with permission). ΔH values, measured by humidity titration calorimetry through Eq. (22), are represented by circles. ΔG values, measured by gravimetry, through Eq. (20), are represented by squares. $-T\Delta S$ values are obtained by difference through Eq. (18). The variations of these state functions vanish for $R_w>5$.

3. Interactions of phospholipid layers with water within the interfacial region

3.1. Repulsive and attractive forces between phospholipid bilayers of a multibilayer stack, mediated by water

Generally speaking, the total force, F, between two surfaces separated by a distance ℓ is determined by the change in Gibbs free energy, G, corresponding to an infinitesimal variation of this distance, at given temperature and pressure [31]:

$$F_{tot} = -(\partial G / \partial \ell)_{T,p}. \quad (23)$$

The sign convention in Eq. (23) is such that repulsive forces are positive. If a volume V of liquid is present in the space between these surfaces, the total force per area of the surfaces represents the osmotic pressure of this liquid, π_{osm}, and, if this liquid is incompressible, it can be written as [31]:

$$P_{tot} = F_{tot}/\text{area} = -1/\text{area}(\partial G/\partial \ell)_{T,p} = -(\partial G/\partial V)_{T,p} = \pi_{osm}. \quad (24)$$

In case of apposing bilayers of a phospholipid/water multibilayer stack, the volume of water within the interbilayer spaces, is equal, per phospholipid molecule, to:

$$V_L = v_w \times n_w = 1/2 A_L \times \ell_w \quad (25)$$

where A_L is the area per phospholipid head, ℓ_w the thickness of the aqueous interbilayer spaces and v_w the molar volume of water. The osmotic pressure π_{osm} can then be written:

$$\pi_{osm} = -1/v_w (\partial G/\partial n_w)_T. \quad (26)$$

Plots of π_{osm} as a function of ℓ_w, for several PCs in various thermodynamical states, have been found to superimpose in the 4 Å $<\ell_w<$ 8 Å range [32]. Therefore, in this ℓ_w range, the predominant interaction between apposing bilayers is of the same kind and qualified hydration pressure, P_{hyd}: $P_{hyd} \sim -\pi_{osm}$ [3,33]. The origin of this pressure is still debated [34–36]. In order to know if protrusion motions of headgroups ([30], Section 2.8) is the cause of the hydration force, Binder et al. [37] have used polymerizable phospholipids for which a cross-linking of polar heads by polymerization prevents such protrusions. As a result, the $P_{hyd}=f(\ell_w)$ plots are superimposed before and after polymerisation (Fig. 5), precluding these protrusions as the cause of the hydration force.

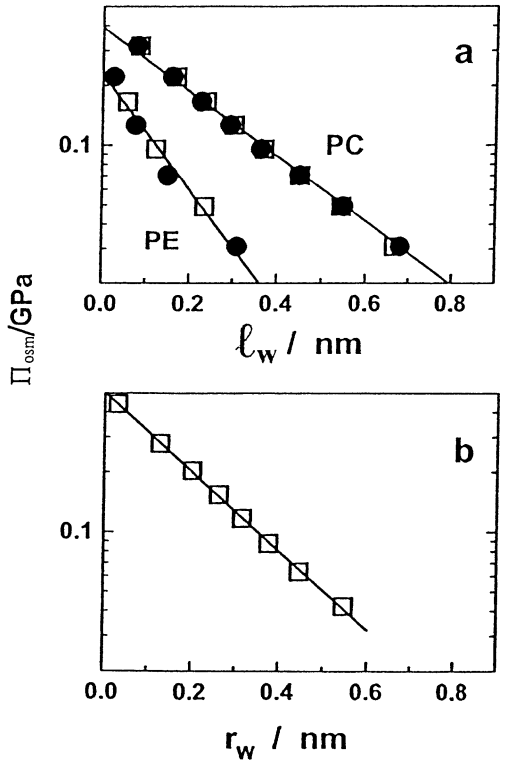

Fig. 5. Variation of the hydration pressure (represented by the "equivalent" osmotic pressure, π_{osm}, Section 3.1) between PC and PE layers as a function of the distance between these layers, ℓ_w or r_w (reproduced from Ref. [37] with permission). (a) apposing bilayers of DTDPC and DTDPE/water multibilayers in the fluid lamellar phase, at 25 °C. (b) DTDPE monolayers delineating water cylinders (of radii r_w) in the H_{II} phase, at 50 °C. In (a) and (b), open squares correspond to monomers and full circles to polymers: the unique regression lines between both types of symbols testify to an independence of the hydration pressure on the polymerization of these phospholipids suppressing protrusion motions of headgroups (cf. text, Section 3.1).

Using the X-ray diffraction/osmotic stress method [12], the function $P_{hyd}=f(\ell_w)$ has been found to have the following phenomenological expression [33]:

$$P_{hyd} = P_0 \exp(-\ell_w/\lambda) \tag{27}$$

where P_0 and λ represent characteristic parameters.

The modification of the variation of the Gibbs free energy of hydration of a phospholipid monolayer in a multibilayer stack, during a variation dV_L of the associated aqueous volume, can be expressed from Eqs. (24)–(27):

$$\begin{aligned} d(\Delta G_{hyd}) &= -dV_L \times \pi_{osm} = dV_L \times P_{hyd} \\ &= 1/2A_L \times d\ell_w \times P_0 \exp(-\ell_w/\lambda). \end{aligned} \tag{28}$$

However, other types of interaction pressures than the hydration pressure have been acknowledged such as: undulation repulsive pressure, P_{und} (due to out-of-plane fluctuations of fluid bilayers), electrostatic repulsive pressure, P_{el} (in the case of charged phospholipids) and short-range steric repulsive pressure, P_{st}. The contributions of these different pressures, based on a Petrache et al.'s [14] analysis of X-ray lines shapes, have been reviewed by McIntosh [38]. They are represented in Fig. 6, as a function of the average thickness of the aqueous interbilayer spacing. These plots indicate that P_{hyd} dominates the repulsive interactions in the 5 Å $<\ell_w<$ 13 Å range. At larger ℓ_w values (and lamellar repeat distances, ℓ), there is a preponderance of the undulation pressure (Fig. 6) whose expression, as a function of T, is [39]:

$$P_{und} \sim (k_B T)^2/(K_c \ell)^2 \tag{29}$$

where k_B is the Boltzmann constant and K_c the modulus of bending rigidity.

3.1.1. Intermembrane structures formed by removal of interbilayer water (stalk hypothesis)

The afore-commented short-range repulsive forces between apposing bilayers can be overcome under certain conditions of hydration, pH, temperature or charge density (in oppositely charged vesicles). In these conditions, for instance, two unilamellar vesicles can fuse: their bilayer membranes merge into one, the rupture of which leads to an exchange of their contents. Information on this fusion process mainly arises from the action of fusogenic proteins on phospholipid membranes [40,41]. However, the lipid composition, especially the incorporation of charged phospholipids into them, is also involved in this process. When neutral planar bilayers pressed out towards each other are subjected to an electric field, the capacitive current of the contact region informs us on its area [42]. Addition of lysolipids, either to the contacting (cis) or to the distal (trans) monolayers, respectively inhibits or promotes the fusion. When two oppositely charged giant vesicles enter into contact in an electrophoretic chamber, hemifusion or full fusion occurs depending on their charge density [43].

The fusion process implies substantial rearrangements of phospholipid and water molecules, especially in the interfacial region. The putative intermediate arrangements of these molecules give rise to warm debates about their free energy and their order of succession (Ref. [41] and references herein). The driving force of these rearrangements probably is not the same according as vesicle membranes are neutral or charged. In case of neutral vesicles, researchers generally agree in recognizing three motifs. In a successive order, first, a necklike structure called stalk (in form of hourglass, Fig. 7B), which connects facing monolayers of apposing bilayers, would be formed. Second, the radial expansion of this stalk, via a lipid diffusion-controlled process, gives rise to a hemifusion diaphragm (called also transmonolayer contact (TMC), Fig. 7C). These TMC can aggregate into stacks of rhomboids [44]. TMC are under stress due to the curvature of contacting (cis) monolayers and to the high free energy of the hydrophobic interstices (stippled areas in Fig. 7C). For a critical value of the tension of the hemifusion diaphragm, TMC can rupture

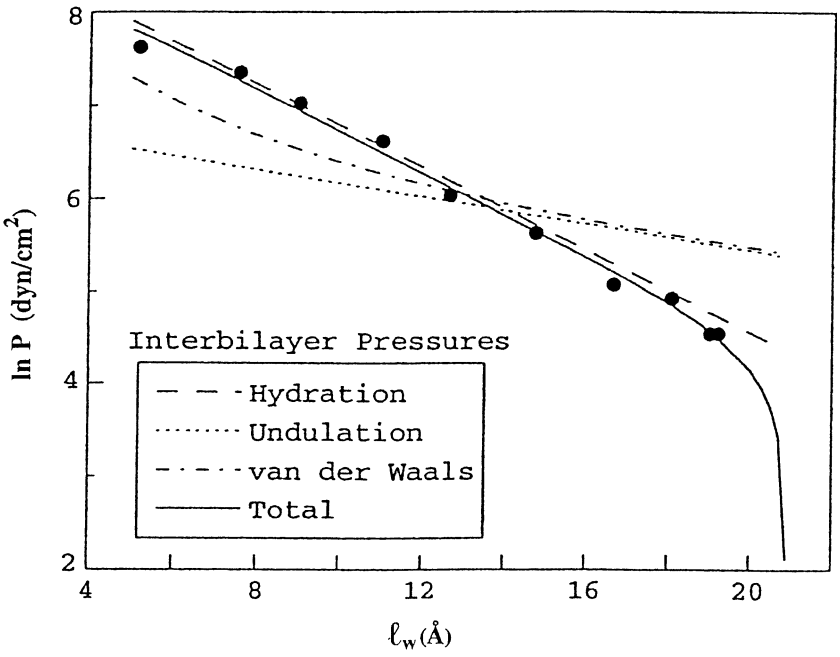

Fig. 6. Plots of the different components of the total pressure P_{tot} between apposing EPC bilayers in the fluid lamellar state, as a function of the thickness of the aqueous interbilayer spacing, ℓ_w (reproduced from Ref. [38], with permission). These different components have been calculated from an analysis of the profiles of the diffraction lines obtained by X-ray diffraction [14]. As shown on this plot, the undulation repulsive pressure between two apposing bilayers dominates, at full hydration, for ℓ_w>12Å.

leading to the formation of a fusion pore (called also interlamellar attachment (ILA)). These ILA resemble to two halves of cylinders of the inverted hexagonal phase, H_{II}, apposed back-to-back. Such an ILA allows the exchange of the contents of fused vesicles. The major impediment opposing to the observation of such intermediate structures is their short lifetime. For instance, TMC arrays with a quasi-hexagonal symmetry have been observed by time-resolved cryotransmission electron microscopy of POPE MLV a few seconds after a pH-jump (triggering the fusion), but the expected corresponding isotropic resonance in ^{31}P-NMR could not be observed after a few minutes [45]. In these circonstances, the recent identification of a stable rhombohedral phase, from X-ray diffraction, for a pure phospholipid like diphytanoylphosphatidylcholine (DPhPC) represents an important breakthrough [46,47]. The corresponding electron density distribution has been found to resemble that of crystals of transmembrane pores formed by intercalating fusogenic peptides into phospholipid multibilayers [48]. The stability of this rhombohedral phase, intermediate between the H_{II} and L_α phases during a RH-controlled hydration, probably arises from the bulkiness of DPhPC fatty chains due to the branchment of methyl groups. As a matter of fact, this bulkiness leads to a favourable negative intrinsic curvature of DPhPC layers (Section 5.2.3).

In case of the fusion of charged vesicles, a recent microfluorimetric imaging method, coupled with fluorescence resonance energy transfer (FRET, Section 2.4) data, has provided an unambiguous proof of the existence of a hemifusion intermediate [43]. Fluorescence spectra relevant to the fusion of two oppositely charged and differently labeled vesicles (DiO-labeled (the donors) and Rh-PE ones (the acceptors)) have been collected by a digital camera. The time-resolved spectral changes, registered as a function of the distance along the fusion axis, have provided information on the diffusion of the fluorescent probes (and, thereby, of phospholipid molecules) during the fusion. Video images, simultaneously but more slowly obtained, demonstrate that, in this case, a flattening of vesicles occurs, creating a tension within the contact region [43]. This tension is increased by the neutralization of the charges borne by each vesicle, and, when exceeding the lysis tension of the contacting bilayer, leads to its breakdown.

3.2. Modifications of the properties of water at the interface of phospholipid layers

The way by which phospholipid monolayers and bilayers affect the state of water at their interfaces includes several structural and thermodynamical properties.

3.2.1. The network of H-bonds is modified

In pure liquid water, the optimal coordination of molecules is tetrahedral and although H-bonds experience unceasing fluctuations of their lengths and angles between them, within randomly formed clusters, they form and break cooperatively. Near a surface or in confined spaces (like the free-volumes within the hydrocarbon region of phospholipid

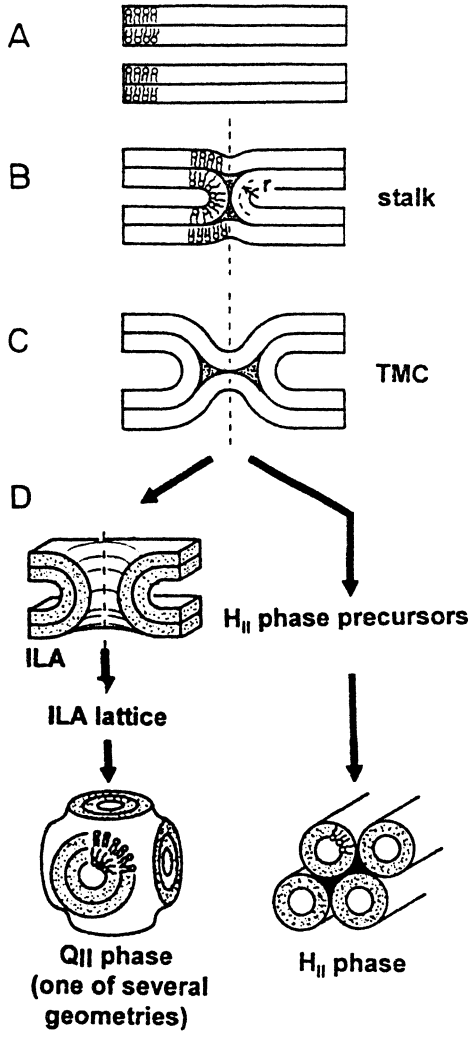

Fig. 7. Intermediate structures postulated by the stalk theory of membrane fusion and inverted hexagonal phase formation from a lamellar phase ([44], reproduced with permission). Phospholipid monolayers are represented as slabs. (A) Apposed bilayers in a multibilayer stack. (B) Stalk formed from phospholipids in the contacting (cis) monolayers. This structure is cylindrically symmetric around the dashed vertical axis. (C) Hemi-fusion intermediate or trans-monolayer contact (TMC). The distal (trans) monolayers form a bilayer hemifusion diaphragm. (D) The rupture of the diaphragm (left) produces a fusion pore or interlamellar attachment (ILA). This step corresponds, for instance, to the fusion of two unilamellar vesicles with mixing of their contents. An accumulation of ILA can lead to the Q_{II} phase. Alternatively, near the $L_\alpha \rightarrow H_{II}$ transition temperature, TMCs assemble to form rhomboids as precursors of the H_{II} phase (right).

bilayers, Section 4.3), this tetrahedral coordination is broken down because H-bonds are formed with phospholipid headgroups and the network of H-bonds is modified. The resulting states of water have properties (density, coordination number, strength and lifetime of H-bonds) different from those in free water.

Information on these different properties has been provided by simulations. First, within a phospholipid bilayer, when approaching the hydrocarbon region, the number of neighbours of one given water molecule decreases, whereas the ability of this molecule of making H-bonds with these neighbours increases [49]. Second, the electrostatic potential due to the charges borne by phosphate and ammonium headgroups leads to an ordering of the dipoles of interfacial molecules. By artificially splitting the contributions of water and phospholipid molecules to the global electrostatic potential, these contributions appear as mirror images [36]. However, the charged headgroups, if projected on the bilayer normal, are at different positions and the resulting charge viewed by interfacial water molecules is negative. Consequently, the water dipoles, although they are quasi-parallel to the interface, point towards the interior region [36,50,51]. It results to a small residual negative potential at the interface, as experimentally measured [52]. A sign reversal of this residual potential is obtained by reducing the hydration level (from $R_w = 11.4$ to 5.4 for DOPC bilayers) [53].

These results convey the idea that *membrane–water interfaces are very rough and diffuse*: at the interface of a phospholipid layer, water is perturbed by up to 1 nm away from it [36].

3.2.2. The water density is increased

The first water molecules sorbed by phospholipids have a molar volume, v_w, smaller than that of the completely H-bonded free water (i.e. 1 $cm^3\ g^{-1}$ or 30 $Å^3$ per molecule). As a matter of fact, during a stepwise phospholipid hydration, sorbed water molecules are successively accommodated in spaces between headgroups and in the interbilayer spacing [54]. The proof of the increased density of phospholipid-sorbed water has been provided by applying a hydrostatic pressure on DOPE membranes in the H_{II} phase [55].

3.2.3. The freezing point of the interbilayer water is depressed

Several results using different methods (RX diffraction [56], DSC [57–62] and Raman spectroscopy [63]) have agreed in establishing *a supercooling of the interfacial water*. This freezing point depression results from the fact that the interbilayer water has an activity lower than 1.

3.2.4. The motional freedom of water molecules is reduced

The dynamics of the orientation of water electric dipoles at the interface of phospholipid layers (either in phospholipid/water multibilayers or in phospholipid-based reverse micelles) has been determined by dielectric spectroscopy (Section 2.6). Sorbed water molecules have a relaxation time different from that of pure water because their orientational mobility is reduced [24]. Recently, Nandi and Bagchi [64], recollecting a lot of dielectric spectroscopy data, on several types of biomolecules, have rationalized them in terms of a dynamic equilibrium between free and H-bonded water molecules in the hydration shell of these biomolecules (Section 3.6).

Generally speaking, the mobility of water molecules confined in small spaces is reduced. The correlation time

(Section 2.2) of motions of the interbilayer water in DOPC/water multibilayers is three times lower at low hydration (narrow interbilayer spaces) than at full hydration [65]. Similarly, water molecules in the core of phospholipid-based reverse micelles, whose dimensions are directly related to R_w, are slowed down when R_w is small enough [66].

This reduction of the motional freedom of water molecules results from their confinement and should not be attributed to their H-bonds with the phospholipid headgroups (Section 3.6). This has been recently confirmed by a study of collective motions of water molecules in nanopores with radii of 1 to 5×10^{-9} m [67]. When the nanopore radius is equal to 1×10^{-9} m, the orientational mobility of enclosed water molecules, compared with free water molecules, is slowed down by a factor of 10.

3.3. Hydration level dependence of the structural parameters of phospholipid/water multibilayer stacks

The thicknesses of the water and phospholipid layers, ℓ_w and ℓ_L, in lamellar phases of phospholipid/water multibilayers, depend on the hydration level. Starting from a slightly hydrated state, these multibilayers swell by addition of water. However, this swelling is not uniform and sorbed water not homogeneously distributed. Especially, in the fluid (L_α) phase, water can accommodate within defects, as identified by freeze-fracture [68]. The presence of such defects leads to an overestimate of the ℓ_w value based on gravimetric measurements, and, consequently, an underestimate of ℓ_L, obtained, from the lamellar repeat distance, $\ell = \ell_L + \ell_w$, measured by X-ray diffraction. In addition, the approximation of non-penetrating water and phospholipid steric layers is coarse. In order to take into account these complications, different methods have been used [12,69]. One of them is developed in the recent Nagle and Tristram-Nagle's review [15]. We will limit ourselves to reproduce their detailed figure (Fig. 8). As shown in the right part of Fig. 8c, the interbilayer water is distributed in two pools, the steric water layer and the water in spaces between phospholipid headgroups comprised, respectively, between $D'_B/2$ and $D/2$ and between D_C and $D'_B/2$. Water molecules within the latter pool represent ~30% of the total, in the fully hydrated DPPC and DMPC gel (L'_β) phases [15,70], against 38% in the fully hydrated DMPC fluid (L_α) phase [70] to be compared with ~50% in DLPE gel and fluid lamellar phases [12,15].

3.3.1. The area per phospholipid molecule is correlated with the interfacial water activity

The area per phospholipid head, A_L, barely different from the area subtended by phospholipid chains, A_{CH}, in phospholipid lamellar phases, reflects important phenomena, as follows.

On the one hand, A_{CH} is linearly related to the average C–D bond order parameter, $-S_{CD}$ (Eq. (1)), determined by ^{2}H-NMR [71]. S_{CD}, in turn, is partially related to the wave numbers of the stretching vibrations of the CH_2 segments of fatty chains (ν_s and $\nu_{as}(CH_2)$, [72,73]). Consequently, a correlation between A_L and these wave numbers is expected. This correlation has been demonstrated by following the effect on FT-IR spectra of either an osmotic stress on fluid DTDPC/water multibilayers, or, a compression of a DMPE monolayer in a Langmuir trough [37]. As shown in Fig. 9b,

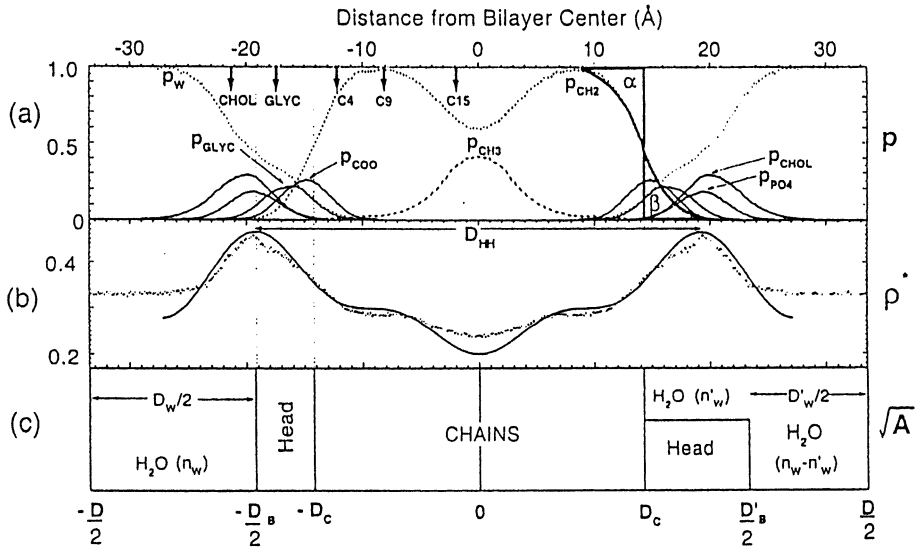

Fig. 8. Three modes of representation of structural data relative to fluid DPPC/water multibilayers (reproduced from Nagle and Tristram-Nagle review [15], with permission). (a) Distribution of the probabilities of occupancy of phospholipid submolecular fragments and interbilayer water molecules along the bilayer normal, p, as a function of the distance from the bilayer center, obtained by simulation [103]. (b) Electron densities profiles, ρ^*, obtained either from X-ray scattering experiments (solid line, [156]), or from simulation (dots, [103]). (c) Volumetric repartition of interbilayer water in two approximations, either non-penetrating phospholipid/water layers (left) or distribution of interbilayer water into two pools (spaces between phospholipid headgroups, and steric interbilayer space, see text, Section 3.3) (right), the scale of abscissas is the same in (a), (b) and (c).

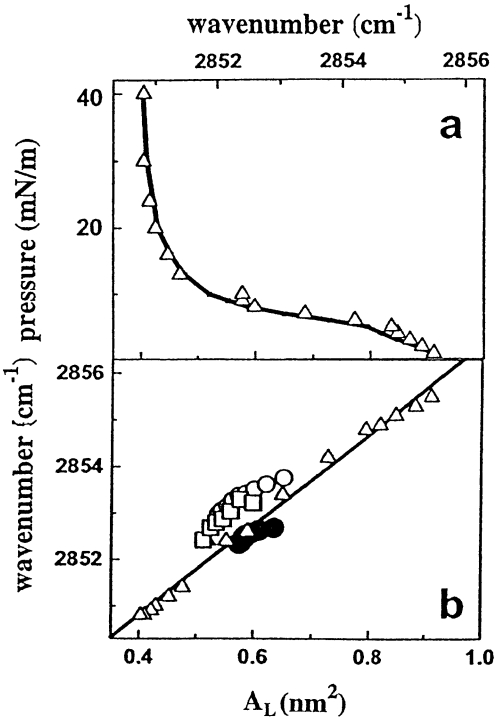

Fig. 9. Illustration of the relation connecting the area per phospholipid molecule in a phospholipid layer, A_L, and the wave number of a spectral benchmark of the degree of order of the phospholipid fatty chains (the maximum of the CH_2 symmetric stretching band, $\nu_s(CH_2)$) (reproduced from Ref. [37], with permission). A_L is varied by applying a lateral pressure either directly, or indirectly, through an osmotic stress. [a] Compression isotherm of a DMPE monolayer, spread at the air–water interface of a Langmuir trough, at 25 °C (line), and wave numbers of the maximum of the $\nu_s(CH_2)$ band, obtained by infrared reflection-absorption in situ (symbols). The curve corresponding to the interpolation of these experimental points is superimposed to the compression isotherm and exhibits an abrupt decrement at the liquid-expanded-solid-condensed transition. [b] Correlation between A_L and the wave numbers of the maximum of the $\nu_s(CH_2)$ band for the previous DMPE monolayer and for DTDPC bilayers under osmotic stress. These latter bilayers were either in a monomeric state (at 10 °C (ρ) and 25 °C (μ)) or in a polymerized state (at 25 °C, full circles).

the maximum wave number of the $\nu_s(CH_2)$ band has been found to be proportional to A_L. The agreement between results obtained for DTDPC multibilayers and DMPE monolayers has additionally demonstrated that a lateral compression due to an osmotic stress has the same effect as a direct lateral compression, namely increasing the degree of order of phospholipid fatty chains.

On the other hand, A_L is linked to the activity of the interfacial water through the lateral tension defined by $\tau = -(\partial G/\partial A_L)_{T,p}$ [74]. As a matter of fact, in the elastic limit of deformation of a bilayer, τ is equal to [74]:

$$\tau = K_a \times (A_L - A_0)/A_0 \quad (30)$$

where K_a is the area compressibility modulus and A_0 and A_L the areas per phospholipid molecule in the fully hydrated state and in a stressed state. Now, τ is related to the work of the osmotic pressure π_{osm}. Using Eq. (28), this work is equal to:

$$d(\Delta G_{dehyd}) = -\pi_{osm} \times dV_L = -1/2\pi_{osm}(\ell_w dA_L + A_L d\ell_w) \quad (31)$$

From the definition of τ, it results:

$$\tau = 1/2\pi_{osm}\ell_w = \pi_{osm} \times R_w v_w/A_L \quad (32)$$

Substituting τ in Eq. (30) and replacing π_{osm} by its expression (Eq. (14)) lead to [74]:

$$A_L = A_0[1 + (RTR_w \ln a_w)/K_a A_0]. \quad (33)$$

Eq. (33) establishes a linear correlation between A_L and a_w (since $\ln a_w \sim 1 - a_w$, as a first approximation, when a_w is around 1). As a matter of fact, such a correlation has been experimentally observed in the range $0.94 \le a_w \le 1$, as shown in Fig. 10-(1) [74]. If the modification of a_w is accompanied by a phase transition, the plot $A_L = f(a_w)$ exhibits a discontinuity (like at $a_w = RH = 0.35$, at 25 °C, for POPC multibilayers, as shown in Fig. 10-(2), [75]).

3.4. Network of H-bonds at the interface of phospholipid layers (from simulations and experiments)

The organization of the interfacial region of phospholipid layers has been studied by experiments [76–79] and simulations [51,80,81]. It differs for PE bilayers from PC ones. During a stepwise hydration, the interfacial water molecules form H-bonds, first, with the PO_2^- headgroup [76,77] and, second, with the C=O headgroups [78]. However, for PCs only, water molecules assemble in the form of a clathrate hydration shell around the hydrophobic $N(CH_3)_3^+$ group [81,82]. Besides, for PEs only, the amine hydrogens, in addition to H-bonds with water, form also H-bonds with the C=O group of the β chain of the same phospholipid molecule [79] and the PO_2^- group of an adjacent phospholipid molecule [51,79,80]. In addition, apposing PE bilayers are linked by bridges of H-bonded water molecules that make shifted with respect to PC ones their π_{osm}–ℓ_w plots (Section 3.1, Fig. 5, [37,83]). As a matter of fact, these bridges prevent the interbilayer spacing from expanding.

Recent simulations have provided important new information on the organization of the interfacial region of fully hydrated fluid phospholipid bilayers [50,84,85]. Intramolecular and intermolecular (between adjacent phospholipid molecules of a same layer) H-bonded water bridges (identified by geometric criteria) link different oxygen atoms (Fig. 11, [84,85]). These bridges form and break unceasingly but if the separation between the two oxygen atoms of interest lasts less than 6×10^{-11} s, they identically reform. Their average lifetime is estimated to over 5×10^{-11} s [84]. In addition, opposite charges borne by

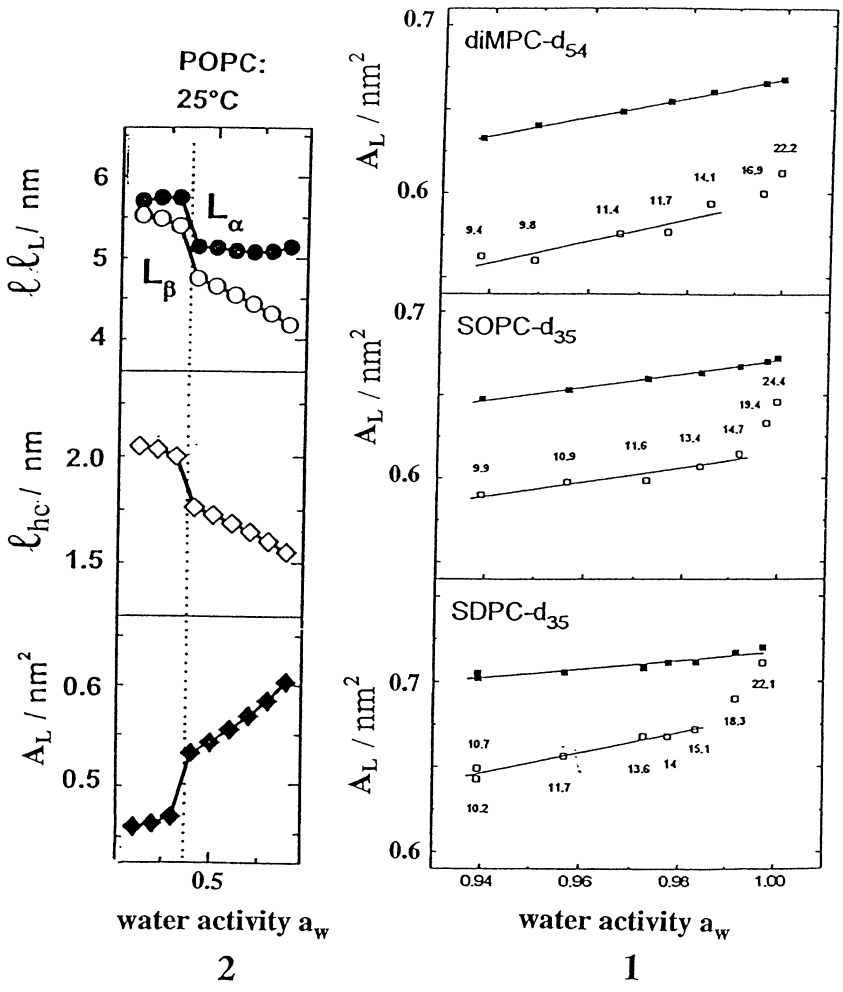

Fig. 10. Illustration of the relation connecting the area per phospholipid molecule in phospholipid/water multibilayers, A_L, and the activity of the interbilayer water, a_w, regulated, either, by the RH of the vapour phase, or by addition of polyethylene glycol to external water. (1) Relation between A_L and a_w for DMPC-d54/water, SOPC-d35/water and SDPC-d35/water multibilayers, at 30 °C, in absence of transition (reproduced from Ref. [74], with permission). The two types of symbols correspond to two methods of calculation of A_L. (2) Plots of A_L, the lamellar repeat distance, ℓ, the phospholipid bilayer thickness, ℓ_L, and the half-thickness of the hydrocarbon region, ℓ_{HC}, as a function of a_w = RH, for POPC multibilayers (reproduced from Ref. [75], with permission). Discontinuities on these plots signal phase transitions.

phosphate and trimethylammonium headgroups of adjacent phospholipid molecules form charge pairings when they are distant from less than 4 Å [85]. These charge pairings, like H-bonded water bridges, form and break with a frequency of 10^{11} s^{-1}. However, the electrostatic interaction remains and, thereby, the lifetime of the charge pairings is as long as 1.4 ns. Finally, 93% *of molecules of a phospholipid layer are linked by charge pairing and* 76% *by water bridging*, thus leading to an interfacial network of short-range attractive interactions.

The presence of such a network of H-bonded water bridges, at the interface of phospholipid layers with water, is confirmed by the interfacial migration of charges observed using Langmuir troughs.

These migrations of charges, at the surface of phospholipid monolayers spread at an air–water interface, have been observed under certain conditions. In a first type of experiments, such a migration has been observed by compressing the monolayer up to a critical value of A_L (60 $Å^2$ corresponding to a distance between polar heads of 8 Å). It is revealed by a jump of the conductance between two parallel electrodes crossing the interface [86]. On the other hand, such a migration has been triggered by injection of protons into a compartment of the trough separated in volume from the subphase [87]. The rate of this migration has been followed owing to a pH-sensitive fluorescent marker. This latter interfacial charge transport has been found to disappear when compressing the monolayer up to the liquid-expanded–solid-condensed transition [87].

In a second type of experiments [88], a purple membrane, containing bacteriorhodopsin labelled by pH-sensitive fluorescent probes, has been flashed on its *extracellular* surface. The resulting protons then migrate along the

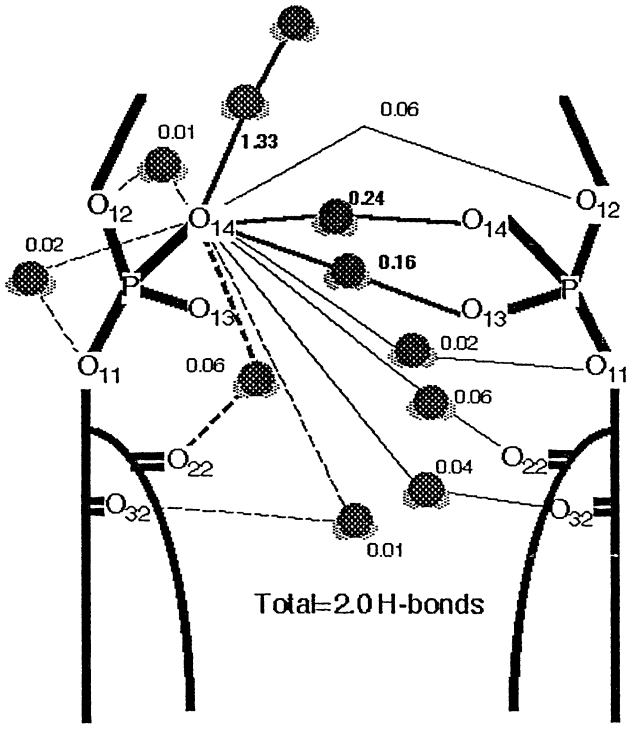

Fig. 11. Overview of the H-bondings of a nonesterified P-oxygen (O_{14}) of a DMPC bilayer, in the fluid lamellar phase, with $R_w = 22.5$, with other oxygen atoms, via water cross-bridges (represented by stippled grey areas). The linked oxygen atoms belong to either the same molecule (intramolecular H-bonding) or adjacent molecules (intermolecular H-bonding) (reproduced from Ref. [84], with permission). The presence of H-bonds has been deduced from geometric criteria by calculations and quantitated in relative values with respect to a total number of 2.

membrane, up to its *cytoplasmic* surface, from which a fluorescent signal is emitted after a certain delay. From this delay, the rate of proton migration has been assessed as 2.6×10^{-3} m s^{-1}.

In a third type of experiments, a phospholipid monolayer is spread in a Langmuir trough whose subphase is a weak acid in which an electrode is immerged [89]. At the surface of this electrode, the acid is reduced. The resulting ion diffuses towards the surface where it deprotonates the phospholipid. The subsequent interfacial migration of charges is revealed by an amplification of the current due to this electrochemical process.

Whatever the actual mechanism of this charge transport from one phospholipid polar head to the adjacent one at the surface of a phospholipid layer (cf. [90] for a discussion of these mechanisms), they require the presence of H-bonded water bridges between the phospholipid polar heads. As a matter of fact, the maximum distance between two atoms to form a H-bond is around 2.8 Å [91], and charge transports have been observed for distances between polar heads as long as 8 Å. The lifetime of such water bridges (5×10^{-11} s) is then sufficient to account for the observed transport rate (2.6×10^{-3} m s^{-1}).

3.5. Coupling and hydration dependence of motions of phospholipid headgroups and interfacial water molecules

The hydration level of phospholipid/water multibilayers has an effect on both the order of orientation and the mobility of interfacial molecules. In addition, this mobility is coupled with that of phospholipid headgroups during changes of temperature. The effects of hydration level and temperature, followed by ^{2}H-NMR [6,7,65,92–94] and dielectric spectroscopy [95,96], will be successively considered below.

Upon increasing hydration, the spin-lattice relaxation rate, $1/T_1$ (the rate of damping of motions, Section 2.2) of D atoms of the choline group of PC bilayers decreases up to a plateau at $R_w = 14–18$. This indicates that this group, as one unit, becomes more mobile [65]. Importantly, after converting R_w into a_w by using sorption isotherms [6], the $1/T_1$ values appear linearly related to a_w for $0.4 < a_w < 1$ [7].

By comparison, the hydration-dependent orientational mobility of the $P^-–N^+$ dipoles is revealed by dielectric spectroscopy (Section 2.6). In case of DMPC/water multibilayers, it increases by a factor of 5, from $R_w = 6$ to $R_w = 15$ [96].

Concerning the interbilayer water molecules of phospholipid/water multibilayers, the degree of order of their orientation is reflected by the ^{2}H-NMR parameter $\Delta\nu_Q$ (Section 2.2). In the fluid lamellar phase, upon increasing hydration at fixed temperature, $\Delta\nu_Q$ decreases whereas the diffusion coefficient parallelly to the interface, $D_{//}$, increases, both continuously [92,93]. Two different interpretations of this result have been given. First, the presence of discrete water shells (with fixed $\Delta\nu_Q$ and $D_{//}$), between which exchanges of molecules occurring in a time short on the time window of ^{2}H-NMR have been assumed [93]. Second, it has been assumed that water molecules are distributed into surface-slowed down and free ones, this distrubution being modulated by the hydration level [92]. After converting R_w into a_w, using sorption isotherms, $\Delta\nu_Q$ values appear linearly related to a_w [6].

Let us now examine the effect of the temperature T, independently to any phase transition. From the temperature dependence of the dielectric relaxation of $P^-–N^+$ dipoles, the energy barrier opposed to their motions has been assessed to 46 kJ mol^{-1} for fluid DMPC bilayers in the fluid lamellar phase [96]. This value is higher than that of the energy barrier opposed to the motions of the single choline group (22 kJ mol^{-1} for fluid DOPC multibilayers, [65]). This difference probably arises from the fact that motions of the phosphocholine, as a whole, require the breakdown of H-bonds with interfacial water molecules.

Concerning interbilayer water molecules, the temperature dependence of their spin-lattice relaxation rate, $1/T_1$, has enabled to assess the energy barrier opposed to their diffusion to around 30 kJ mol^{-1} in the fluid lamellar phase [93,94], to be compared with 21 kJ mol^{-1} for the self-diffusion of pure water.

A coupling between the motions of phospholipid headgroups and the sorbed water molecules in gel and subgel phases has been evidenced. In several phospholipid/water samples, abrupt changes of the ^{2}H-NMR spectra of unfrozen water [97,98] and the ^{31}P-NMR spectra of the phosphate headgroups [98] have been observed at the same temperature T (the temperature of homogeneous nucleation of ice, $T=40$ °C). This result suggests that the unfrozen water molecules could be those bound to the phosphate group.

If, upon increasing T, a phase transition occurs, the order of phospholipid-sorbed water molecules abruptly changes. As an example, the ^{2}H-NMR spectra of water molecules of DPPC/water multibilayers display two different $\Delta\nu_Q$ for $T<T_m$ and $T>T_m$, where T_m is the temperature of the gel (L_β') → fluid (L_α) transition ([94], Fig. 12).

Finally, all these changes of the ^{2}H-NMR parameters of phospholipid/water samples, as a function of the temperature and the hydration level, have led Ulrich and Watts to the following conclusion [7]. Phospholipid headgroups and sorbed water molecules, in the interfacial region of not fully hydrated phospholipid/water multibilayers, form a single phase thermodynamically governed by the activity of interbilayer water. Their motional freedom is facilitated by the swelling of polar heads upon increasing hydration, which is reflected by the gain of entropy accompanying the hydration of a phospholipid (Section 2.8).

3.6. Dynamic character of the H-bonding between phospholipid headgroups and interfacial water

Two facts give to the H-bonding between phospholipid headgroups and interfacial water molecules a dynamic character. First, H-bonds have a short lifetime ($\tau_H \sim 10^{-10}$ s, Section 3.4, [84]). Second, the rate of exchange of interfacial water molecules depends on their confinement (Section 3.2.4). Consequently, the turnover of water molecules near phospholipid headgroups, during their mutual H-bonding, is governed by the following equilibrium:

$$[H_2O]_{pool}^{(\tau_{ex})} \rightleftarrows_{(\tau_H)} [H_2O]_{H-bonded}. \quad (34)$$

In Eq. (34), τ_{ex} denotes the delay for reforming a H-bond after its release, by exchange of water molecules. The recognition of this equilibrium originates from two types of studies on phospholipid-based reverse micelles: the measurement of the dielectric relaxation of endomicellar water ([64], Section 2.6) and the study of the solvation dynamics of a fluorescent probe dissolved in this water ([99], Section 2.4). From the latter studies, the orientational mobility of endomicellar water molecules and, thereby τ_{ex}, depends on R_w which governs the size of micelles. However, this dependence is specific to each type of micelles. In case of EPC/water/cyclohexane reverse micelles [66], the following values have been obtained: at $R_w=4.8$, $\tau_{ex} \geq 5\times10^{-10}$ s whereas at $R_w=5.8$ and 6.8, much smaller values, equal, respectively, to 1.5×10^{-11} and 5×10^{-13} s, have been sequentially obtained. It is worth noting that the τ_{ex} value corresponding to the smaller micelles agrees with the correlation time (Section 2.2) of interbilayer water molecules in barely hydrated DOPC/water multibilayers ($\tau_c \sim 3\times10^{-10}$ s, [65]).

The equilibrium represented by Eq. (34), can be revealed by FT-IR spectroscopy, the most suitable method to identify H-bonds (Section 2.3). The achievement of a FT-IR spectrum (the cumulation of a lot of interferograms) takes a time, τ_f, much larger than τ_{ex} and τ_H. Consequently, the identification of permanent or not H-bonds, from FT-IR spectra, depends on the compared magnitudes of τ_{ex} and τ_H time intervals within the much larger τ_f time interval. Such a comparison is shown in Fig. 13, taking, for τ_{ex}, the values obtained for EPC/water/cyclohexane micelles [66], and, for $\tau_H \sim 10^{-10}$ s (Section 3.6, [84]). According to the size of micelles (the magnitude of R_w), it should result a quasi nothing-to-all appearance of H-bonds. As a matter of fact, for small micelles ($\tau_{ex} \sim 10^{-9}$ s $\sim 10\tau_H$), the H-bonds are effective for 10% of τ_f whereas for large micelles ($\tau_{ex} \sim 10^{-11}$ s $\sim \tau_H/10$), the H-bonds are effective for 90% of τ_f. This interpretation has been confirmed by a study of DPPC/D_2O/pyridine reverse micelles as a function of R_w (Milhaud and Chassenieux, 2003, unpublished work). The perenniality or not of the H-bonds between D_2O molecules and the phosphate headgroup has been visualized, on the micelle FT-IR spectra, by the observation or not of a downshift of the $\nu_{as}(PO_2^-)$ band (Fig. 13). A nothing-to-all appearance of such a shift (a nothing-to-all presence of these H-bonds) has been observed in a small interval (from 25 to 33) of R_w values. However, the size of these micelles appears constant, as measured by dynamic light scattering. This apparent contradiction has received the following interpretation. At $R_w \leq 25$, the small micelles would aggre-

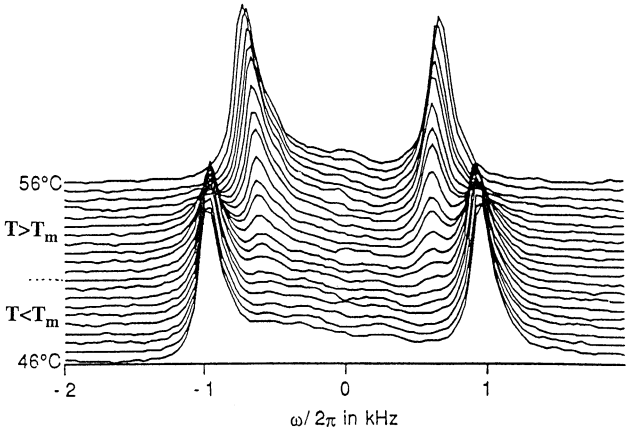

Fig. 12. ^{2}H-NMR spectra of sorbed water demonstrating the coupling of the states of phospholipid and sorbed water molecules, in oriented DPPC/ D_2O multibilayers with $R_w=9$. Spectra are represented at intervals of 0.5 °C, in a temperature range (from 46 to 56 °C) encompassing the gel (L_β') → fluid (L_α) transition temperature, T_m ($T_m=51$ °C from DSC measurements) (reproduced from Ref. [94], with permission). The quadrupolar splittings of these spectra (Section 2.2), reflecting the degree of order of the sorbed water molecules, differ at $T<T_m$ and $T>T_m$. However, in a range of 3–4 °C around T_m, these two ordering states coexist.

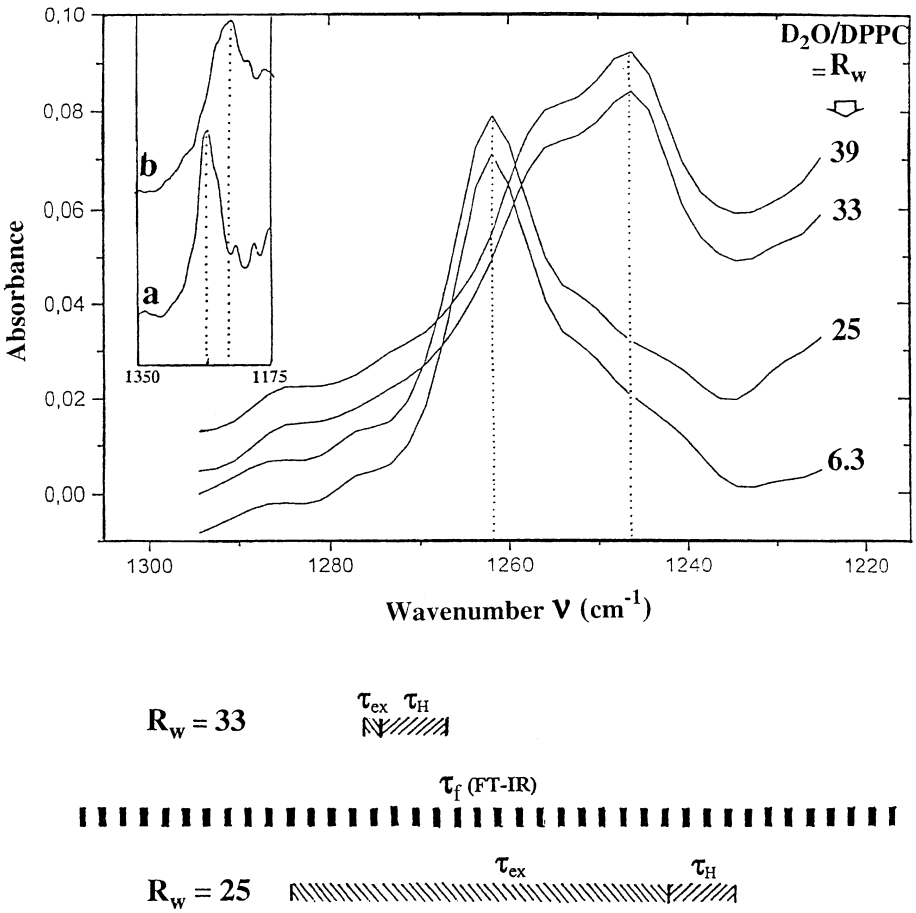

Fig. 13. Top: FT-IR difference spectra of DPPC/D_2O/pyridine reverse micelles (after subtraction of the pyridine spectrum) showing the PO_2^- asymmetric stretching band ($\nu_{as}(PO_2^-)$) at different D_2O/DPPC molar ratios, R_w (Milhaud and Chassenieux, unpublished results). An abrupt downshift of this band is observed by increasing R_w from 25 to 33, signalling the formation of H-bonds between these PO_2^- headgroups and water molecules (see text, Section 2.3). Spectra are vertically displaced to show the details of their contours. Insert: contours of the $\nu_{as}(PO_2^-)$ bands of FT-IR spectra of anhydrous (a) and fully hydrated (b) DPPC/water samples (adapted from Ref. [76] with permission). Bottom: Comparison of the three time intervals implied in the observation of these H-bonds: (i) lifetime of H-bonds ($\tau_H \sim 10^{-10}$ s, [84]). (ii) Delay for reforming these H-bonds, after their release, by exchange of water molecules, τ_{ex} (depending on the size of micelles, [66]). (iii) Duration of the cumulation of spectra, τ_f (~ 30 s), represented by a lot of 10^{-14} s long observation windows (black rectangles). At $R_w = 25$ (small aggregated micelles), $\tau_{ex} \sim 10^{-9}$ s ~ $10\tau_H$: the H-bonds are effective for 10% only of τ_f. At $R_w = 33$ (big micelles formed by fusion of aggregated micelles), $\tau_{ex} \sim 10^{-11}$ s ~ $\tau_H/10$: the H-bonds are effective for 90% of τ_f. These two different situations would be responsible for a nothing-to-all appearance of H-bonds. The actual scale of these different times is not respected.

gate into a big object and, at R_w around 30, these aggregated micelles would abruptly fuse into one big micelle. The resulting freeing of the motions of endomicellar water molecules (a percolation threshold) would lead to a drop of τ_{ex} and, thereby, a sudden emergence of H-bonds. This result would confirm that the slowing down of water molecules in restricted environments instead of being due to their H-bonding (since no H-bond appears under particular conditions) is due to their confinement.

4. Interactions of phospholipid and water molecules within the hydrocarbon region of bilayer membranes

Within the hydrocarbon region of phospholipid bilayers, it is still acknowledged that the presence of water is questionable in absence of transmembrane water flux generated by a transmembrane gradient of the water chemical potential (Section 2.7, Eq. (11)). However, experimental and theoretical results, commented below, demonstrate that water molecules actually penetrate into this region.

4.1. Probabilities of occupancy of water molecules and phospholipid submolecular fragments along the normal to a multibilayer stack

Combination of X-ray and neutron diffraction data have enabled to obtain, with computer-aided fitting, a complete picture of fluid model membranes (Section 2.1, [13]). Following the pioneering White and Wiener's work, atomic-level calculations have allowed this fitting to be refined. Optimal volumes of the phospholipid submolecular fragments have been obtained from electron density profiles of several phospholipid/water multibilayers [100–103] by as-

suming that they are independent of both the position of these fragments along the normal to a bilayer and the hydration level and by ensuring the conservation of the global volume.

As an example, represented in Fig. 14A and B are the distributions of the probabilities of occupancy of water molecules and phospholipid submolecular fragments of a moderately hydrated DOPC/water multibilayer ($R_w = 5.4$, RH = 0.66). These pictures appeal two remarks. First, the boundary between apolar and polar regions of a bilayer is located at the level of ester groups, in agreement with an earlier analysis of X-ray structural data [70]. Second, the distributions of the probabilities of occupancy of water molecules and methylene groups overlap (Fig. 14B).

4.2. The presence of water within the hydrocarbon region of phospholipid bilayers in the fluid lamellar phase has been established

As suggested by the above representation, the penetration of water down to the hydrocarbon region of a fluid bilayer is supported by results of fluorescence experiments.

In a first type of experiments, a fluorophore, introduced into the hydrocarbon region of a fluid EPC bilayer, excited by a light pulse, exhibits a time-resolved emission spectrum revealing the occurrence of a protic environment [104]. In a second type of experiments, the presence of water in the hydrocarbon region of membranes of DPPC LUV has been found to depend on their thermodynamical state, as studied by wavelength-selective fluorescence (REES effect, Section 2.4, [105]),. Two fluorophores differently located within these membranes (F_{if}, within their interfacial region, or, F_{it}, within their hydrocarbon region) depending on their location exhibit or not a REES effect in their emission spectra. F_{if} spectra exhibit a REES effect whatever the thermodynamical state of membranes, in agreement with the abundant presence of water in the interfacial region. In contrast, F_{it} spectra exhibit a REES effect only when the LUV membranes are in the fluid lamellar state. In gel phase, it is probable that water molecules are too fewer so that they can be detected.

4.3. Modulation of the water transport across a bilayer membrane by its free-volume properties

Free-volumes able to accommodate water molecules within the hydrocarbon region of phospholipid bilayers are defects in the packing of fatty chains. Within these fatty chains the torsional states of dihedral angles are triple (trans (t, 180°) and ± gauche (g, ± 60°)) and defects are formed by sequences of these torsional states, such as kinks ($g^+ t g^-$ and $g^- t g^+$) and jogs ($g^+ t t t g^-$ and $g^- t t t g^+$). The probabilities of presence of such defects have been deter-

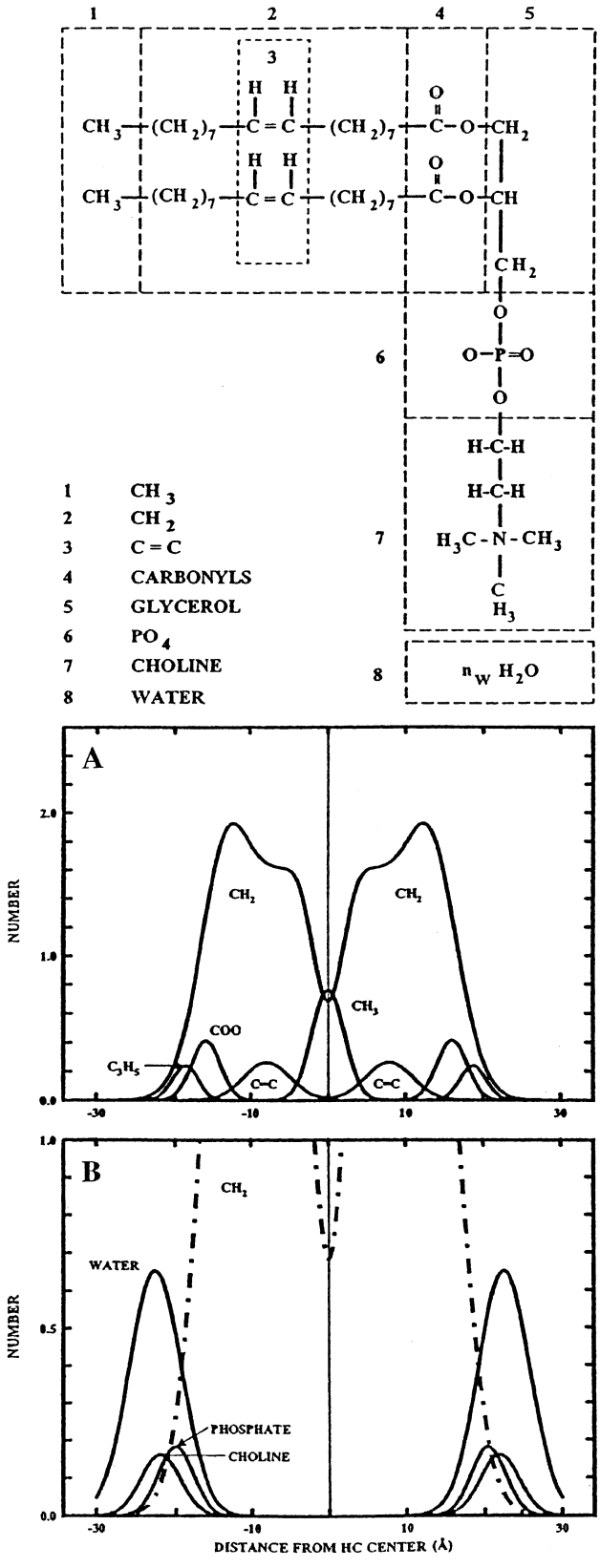

Fig. 14. Illustration of the method of computer-aided refinement of X-ray and neutron diffraction data, in case of poorly hydrated (RH = 0.6) DOPC/water fluid multibilayers (reproduced from Ref. [13], with permission). The DOPC molecules are subdivided into fragments (top). The probabilities of occupancy of these fragments along a bilayer normal are represented by distributions whose widths reflect the amplitude of the thermal motions (bottom). The hydrocarbon (A) and interfacial (B) regions are represented at two different scales of ordinate.

mined by calculations [106] and experiments [107]. They are less present in the gel phase than in the fluid lamellar phase. In the latter case, their presence leads to an increase of the lateral diffusion coefficient (parallelly to the interface) of phospholipid molecules (Section 3.5).

Let us now examine the implication of these defects in the transbilayer transport of a solute like water. First and foremost, let us emphasize that the permeability coefficient relevant to the transport of water ($\sim 10^{-4}$ m s^{-1} in the fluid lamellar phase) is 10^4 higher than the corresponding ones for different small neutral solutes [108]. Two models of transport are generally distinguished. In the solubility-diffusion model [108,109], a phospholipid bilayer is considered as an ℓ_L-thick hydrophobic slab and the permeability coefficient, P_{th} cm s^{-1}, written as:

$$P_{th} = KD/\ell_L \quad (35)$$

where K is the partition coefficient of the solute and D its diffusion coefficient. In the second model, the transport is visualized as a hopping from a transient defect to another one in the hydrocarbon region [110]. It is supported by the 10^2 times increase of the water permeability coefficient at the main transition temperature. Before discussing the respective merits of these two models, we will refer to the earlier "kink model", elaborated by Galla et al. [111], which reconciles them.

Galla et al.'s model is based on a correlation between experimentally measured rate of the *lateral* displacement of a solute (assumed as accommodated in a kink of a phospholipid fatty chain) and the rate of the *transversal* migration of a kink along this chain. Fluorescent probes, able to form excimers, have been incorporated into phospholipid bilayers and their lateral diffusion coefficient measured. These coefficients have been found not to depend on the length of the fatty chains and the head group nature but to depend exponentially on the temperature. Their values have been compared with those resulting from a classical free-volume model. In case of phospholipid bilayers, free-volumes between two adjacent fatty chains are created by the presence of a kink. During the forwarding lateral diffusion of one chain containing a kink, the corresponding free-volume is transmitted to the rear one and so on during the transversal migration of this kink: lateral and transversal displacements of free-volumes are coupled [111]. If a solute is nested in such a free-volume, its transbilayer transport will be related to its lateral displacement. Supporting this model, the known value of the energy barrier opposed to the transversal migration of a kink has allowed to reproduce the experimentally measured lateral diffusion coefficients of the fluorescent probes incorporated into the bilayers. Finally, Galla et al. [111] have replaced the notion of free-volume by that of free-area disposable within the area subtended by fatty chains, A_f, whose temperature dependence is:

$$A_f = \alpha \times A_0(T - T_0). \quad (36)$$

In Eq. (36), T_o and A_0 denote the temperature and the area per molecule in the crystal state, and α the lateral thermal expansion coefficient. The transbilayer transport of a solute exponentially depends on the so-defined A_f [111].

In the following, will be successively commented calculations on the distribution of free-volumes within a fluid lamellar bilayer and their applications to the transport phenomena. From simulations, both Marrink et al. [112] and Xiang [106] have shown that the distribution of free-volumes along the normal to a phospholipid bilayer is complementary to the distribution of its electron density. It exhibits a maximum at the center of the bilayer corresponding to the minimum of electron density. In addition, within this center, the free-volumes are interconnected (the percolation threshold is reached, [112]), allowing water molecules to be accommodated in a specific arrangement. As a matter of fact, simulations have revealed that the ordering state of such internal water molecules is very specific (Section 3.2.1, [49]). In the hydrocarbon region of phospholipid bilayers, the fraction of the neighbours of one given water molecule, being H-bonded to it, increases from 0.56 (in free water) to 1: water molecules are there *in the form of H-bonded single-file strands*. Supporting such an arrangement of water molecules, recent simulations have shown that, in 8-Å-diameter carbon nanotubes, chains of H-bonded water molecules can stay in equilibrium with external free water [113].

Applications of such calculations to the transbilayer water transport have been made by the two same groups of authors. On the one hand, Marrink and Berendsen [49] have used a four-region model of phospholipid bilayers and calculated the rate of transport of one water molecule constrained in this model. The main resistance opposed to this transport has been found to be the region located between the glycerol backbone and the end of chains. On the other hand, Xiang and Anderson [114] have measured the permeability coefficients of acetic acid, under different conditions, and analysed them by a semi-empirical solubility-diffusion model, applicable to the water transport. The factor f by which the effective permeability coefficients, P_{eff}, are reduced with respect to the theoretical ones, P_{th} (Eq. (35)) has been found to depend on T and the difference $A_L - A_0$ (the free-area). This approach amounts to reduce the kinetics of the water transport to its rate-determining step, i.e. the crossing of the chain region in the Marrink and Berendsen's model [49]. The dependences of the water permeability coefficients on T and free-area, obtained by Xiang and Anderson, agree with Galla et al.'s [111] and with recent results [115]. The influence of T on the transmembrane water transport has been recently directly measured using giant unilamellar vesicles (GUV) [115]. GUV were prepared from polyunsaturated phospholipids for which the room temperature, T_r, corresponds to different reduced temperature, $T_{red}=(T_r - T_m)/T_m$. These GUV were transferred into a hypotonic medium where they swelled by penetration of

water. From the rate of this penetration at T_r, the corresponding water permeability coefficient has been found to exponentially depends on T_{red} [115].

Finally, how does the transmembrane transport of water work when an osmotic stress is applied to a membrane? It proceeds in two steps. First, the application of a transbilayer gradient of water chemical potential from external water (compartment I in Figs. 2 and 3) to the internal one (compartment II in Figs. 2 and 3) triggers a water outflux (Section 2.7, Eq. (11)). It results to dehydration of the phospholipid and lateral compression [37], leading to a straightening of fatty chains and, thereby, to a reduction of the free-area. Second, this area constriction restrains the transport of water as afore-described (Eq. (36), [114]). Finally, the rupture of the equilibrium following from the applied osmotic stress leads to two opposed tendencies which counterbalance. The emerging quasi-equilibrium corresponds to an increase of the order of fatty chains (owing to the relation between the order parameter and the area per phospholipid molecule [71]) and a reduction of the hydration level. This transformation has been called a lyotropic chain-ordering transition. We will give further examples of such transitions (Section 5.3.2).

5. Coupling of the thermodynamical states of phospholipid and sorbed water molecules in phospholipid/water samples during phase transitions

5.1. Phase diagrams

Phase transitions are controlled by thermodynamical and kinetic factors [116]. The thermodynamical driving force of a transition, from phase I to phase II, is the difference of their Gibbs free energy, ΔG_{I-II}. In case of lamellar-to-lamellar phase transitions for which the water–phospholipid membrane interface is flat, ΔG_{I-II} is only due to the different hydration states (different activities of interbilayer water, a_w^{II}, leading to different values of R_w, Section 2.8). When a_w^{II} is controlled by the RH of the surrounding gas phase (humidity-controlled osmotic stress, Section 2.7), the two variables determining the domains of stability of each thermodynamic phase of a phospholipid/water sample (the phase diagram) are therefore RH and T. In earlier reviews [117–119], phase diagrams were given as function of R_w and T. A derivation of RH-T phase diagrams from these R_w-T ones requires to know the sorption isotherms, $R_w = f(\mathrm{RH})$, which are known only for a few phospholipids: DMPC [5,26], DLPC [5], DOPE [120], DODPC [120], POPC [75] and SDPC [75] and some ones are reproduced in Fig. 15. In case of lamellar-to-inverted hexagonal phase transitions, additional terms of the Gibbs free energy come into play.

Concerning the kinetics factors acting on phase transitions, they depend on the occurrence of transient intermediates. If intermediates with free energies higher than those of the initial states exist, the rate of the transition can be written like in the transition state theory [121]:

$$\text{Rate } \alpha \exp(-G^{\neq}/RT). \tag{37}$$

In Eq. (37), the free energy of activation, $G^{\neq}$, corresponds to the energy barrier to overcome for forming nonequilibrium intermediates. Such transient intermediates can be identified owing to the coupling of jumps in temperature or pressure (Refs. [116,122] and references herein) with time-resolved X-ray diffraction using synchrotron radiation ([123], Section 5.2.3). Such sophisticated methods have been elsewhere reviewed [124].

5.2. Thermal transitions

5.2.1. Chain-melting, sub-main and main transition and pretransition

The chain-melting, L'_β (gel) $\rightarrow L_\alpha$ (fluid), transition, occurs at a temperature, T_m, which depends on the hydration level of the phospholipid sample, as shown by numerous results on saturated [125] and unsaturated PCs [61] and PEs [126,127]. This hydration dependence of T_m is a consequence of the lateral compression exerted when withdrawing the interbilayer water (Fig. 9, [37]). But, in fact, rather than depending on R_w, T_m depends on the space-averaged activity of interbilayer water which controls R_w and the tightness of the chain packing (the area per phospholipid molecule, Section 3.3). This water-activity dependence is confirmed by the linear relation, established by Kodama et al. [128], between T_m and the proportion of interbilayer unfreezable water molecules (since the freezing temperature of water is directly linked to its activity).

An examination of the events occurring around T_m necessarily implies to speak of the pretransition (L'_β (gel phase) $\rightarrow P'_\beta$ (rippled phase) and the sub-main transition occurring a few degrees below T_m. As a matter of fact, as recently modelled by Heimburg [129], these two transitions are different manifestations of the same cause, namely the thermally induced melting of fatty chains in a fraction of phospholipid molecules. The corresponding creation of point defects requires rearrangements for minimizing the overall free energy. First, the point defects are gathered into one-dimensional line defects. Second, such a line defect, if present within one monolayer of a phospholipid bilayer, leads to: (i) a bending of the interface of this monolayer (due to the change of area per phospholipid molecule); (ii) modifications of the interactions between adjacent phospholipid molecules and phospholipid and water molecules. These latter modifications differ accordingly as they occur in the convex or the concave segments of the monolayer. They lead to a gathering of line defects in domains generating the formation of periodic ripples characteristic of the P'_β phase. This phase would be a mixture of phospholipid molecules in the L'_β phase (with the smaller area per

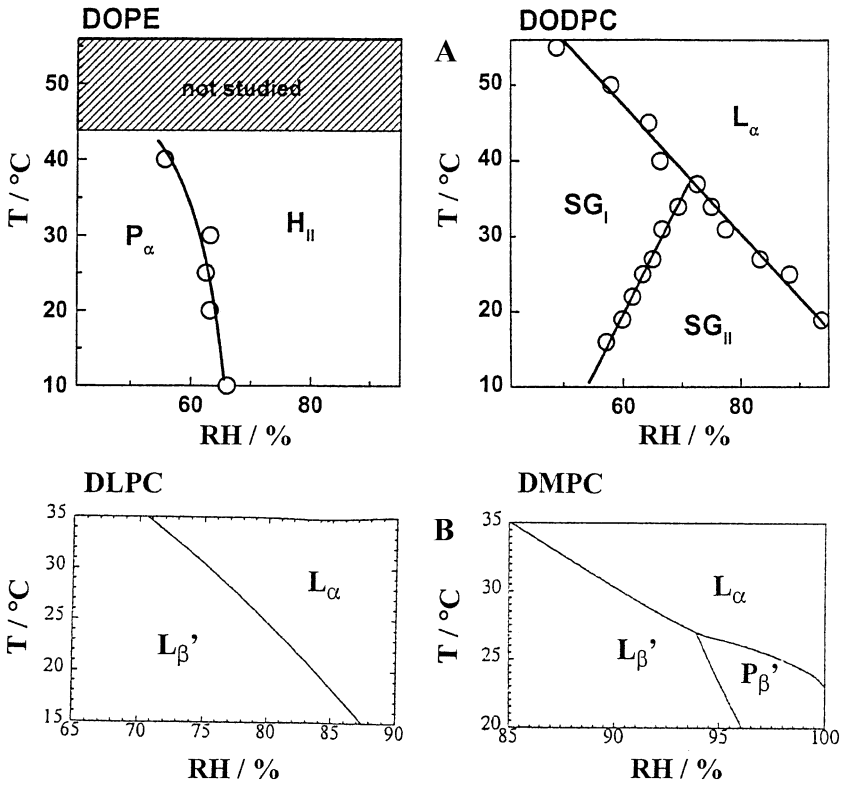

Fig. 15. RH-T phase diagrams of DOPE and DODPC (adapted from Ref. [120], with permission) and of DLPC and DMPC (adapted from Ref. [5], with permission). For DOPE and DODPC phase diagrams, the structural information has been provided by FT-IR spectroscopy (symbols represent experimental data and solid lines interpolations between them). For DLPC and DMPC diagrams, the boundaries between the different states result from microcalorimetric data (obtained with a special calorimeter enabling to measure simultaneously the variation of the Gibbs free energy, and that of the partial enthalpy of water during the sorption of water by the phospholipid [28]).

molecule), gathered into concave segments of each monolayer, and phospholipid molecules in the L_α phase gathered into convex segments. Owing to this model, Heimburg could have built the variation of the heat capacity of a DPPC /water sample, upon a heating responsible for these modifications. The corresponding simulated thermograms exhibit two endotherms, attributed to the pretransition and the main transition, and no decrease down to the baseline between them.

This model has been confirmed by two types of experiments. First, fluorescence measurements [130,131] have evidenced the co-existence of phospholipid molecules in the L_α and the L'_β phases, in the range $T_p < T < T_m$ (where T_p is the pretransition temperature) and their segregation in domains. Fluorescent probes, able to form excimers, were incorporated into DMPC LUV membranes. By heating these LUV, the ratio of the fluorescent intensities of excimers and monomers has been found to go to a maximum at $T_m - 2$ °C [131]. This result has been interpreted as the formation of excimers at the boundaries of fluid domains in the gel bulk. These boundaries would reach their maximum in length 2 °C before T_m [130] while, at T_m, they would disappear for the benefit of a highly cooperative lattice, preventing excimers to be formed [131]. The second type of experiments confirming the Heimburg's model consists in time-resolved experiments [132]. DPPC/water multibilayers were heated by a T-jump, up to a temperature T in the range $T_p < T < T_m$, and their relaxation followed by X-ray diffraction. This relaxation occurs in two steps. First (in a time shorter than 1 s), an intermediary phase, called L^*_α (with disordered fatty chains but with interbilayer aqueous spaces as thin as in the L'_β phase), is formed. Second (in a time of 3s), phospholipid molecules in this L^*_α phase, and in the L'_β phase, would transform into the P'_β phase, by interaction with neighbouring water molecules (interdependence of their chemical potentials, Section 2.7). As a matter of fact, for minimizing the overall free energy, water molecules should be redistributed and this slow redistribution controls the T-jump-induced $L_\alpha \rightarrow P'_\beta$ transition [132].

The sub-main transition, occurring in the range $T_p < T < T_m$, for long chain (with more than 16 C atoms) only phospholipids, testifies to the slowness of such a redistribution of water molecules within a sample prepared by hydrating a dry phospholipid with liquid water. At the corresponding transition temperature, phospholipid molecules in the L_α phase and in the P'_β phase are both present, as demonstrated by X-ray diffraction experiments [133]. The corresponding endotherm is very narrow, reflecting a

high cooperativity. This suggests that this transition implies a complete equilibration of water and phospholipid molecules within the sample. As a support, the surface of this endotherm increases by prolongated incubation of the samples after their preparation [134]. To sum up, the relaxation of a phospholipid/water sample after a heat perturbation a few degrees below T_m implies slow rearrangements of phospholipid and water molecules, reflected by the pretransition and the sub-main transition. These two transitions have no isothermal lyotropic equivalent, which confirms that they are due to a rearrangement of water and phospholipid molecules after a heat-induced creation of defects within the chain packing.

Upon approaching T_m from T_m+2, an anomalous increase of ℓ occurs for PC multibilayer stacks [39]. This anomalous increase is only partially explained by an increase of ℓ_L [135]. The remaining "unexplained" 2-Å increase results from an increase of ℓ_w, as recently demonstrated by X-ray diffraction [136]. Analysing the profiles of the diffraction lines, whose tails depend on a fluctuation parameter (Caillé parameter) related to the bilayer modulus of bending rigidity, K_c, and the bulk modulus of compression, B, Pabst et al. [136] have evidenced an increase by 10% of this parameter (a reduction of K_c and B) within this range of temperature. The consequential increased flexibility (softening) of bilayers generates undulations of their interfaces (Section 3.1), which would be the cause of the anomalous increase of ℓ_w. A confirmation of this interpretation has been given by Pabst et al. [136] by neutron diffraction experiments under osmotic stress. The anomalous swelling has been found to be almost entirely suppressed by an osmotic pressure of 16 atm, sufficient for rigidifying the interfaces.

5.2.2. Subtransition

The formation of the subgel or crystal phase, L_c, requires cold incubations, especially prolonged in case of saturated phospholipids [59,62,137]. During them, interactions arise between phospholipid and interfacial water molecules, as reflected by the DSC thermograms. These interactions differ according to the range of the corresponding transition temperature, T_c. If $T_c>0$ °C, these interactions induce the formation of shoulders on the low-temperature side of the water melting endotherm ([59], Fig. 16).

If $T_c<0$ °C, the chain melting (L_β (gel) → L_α (fluid) or L_c (crystal) → L_α (fluid)) occurs in the presence of frozen water. In case of DOPC/water multibilayers ($T_m=-16.5$ °C), it results to a broad endotherm encompassing the range, -16.5 °C $<T<0$ °C, and, when increasing their hydration level, this endotherm shifts progressively up to 0 °C [61]. Ulrich et al.'s interpretation of this fact is that sorbed frozen water molecules melt by contact with fluid DOPC bilayers because of the lessening of their chemical potential (because the affinity for water in the L_α phase is higher than in the L_c phase). These melted water molecules exchange one another with freezed free ones with a rapidity

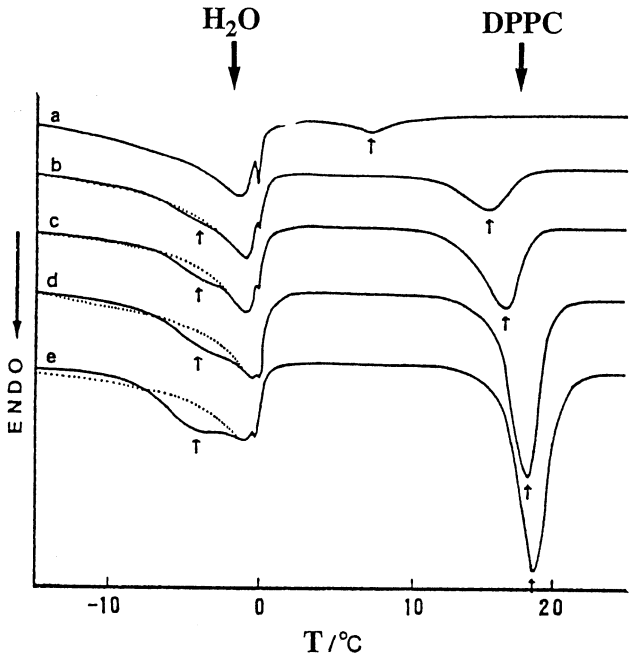

Fig. 16. DSC recordings showing the phospholipid and water endotherms of DPPC/water multibilayers as a function of the duration of a cold incubation applied to transform the gel phase into the subgel one (storage at −20 °C for Δt hours, (a): $\Delta t=0$; (b): $\Delta t=17$; (c): $\Delta t=24$; (d): $\Delta t=72$; (e): $\Delta t=96$) (reproduced from Ref. [59], with permission). The interdependence of the thermodynamical states of phospholipid and water, during this cold incubation, is revealed by the parallel evolutions of these endotherms. When Δt increases, the surface of the phospholipid endotherm enlarges whereas the ice-melting endotherm exhibits an increasing shoulder on its low-temperature side. The dotted lines correspond to the nontreated sample.

depending on the strength of their H-bonds with headgroups, i.e. the hydration level (Section 2.8). If this exchange is fast on the time window of DSC (1 °/min), a single water endotherm results whose temperature increases up to 0 °C, by increasing the hydration level. These results confirm the presence of several populations of differently H-bonded water molecules in the interbilayer spaces (Section 3.2.2). The exchange of molecules between these populations depends on the mobility of phospholipid headgroups which itself depends on the hydration level of the phospholipid (Section 3.5, [7]).

5.2.3. Lamellar fluid (L_α) to inverted hexagonal (H_{II}) transition

Some phosphatidylethanolamines are prone to form nonlamellar phases, like the inverted hexagonal (H_{II}) phase (phase II), by heating and/or dehydrating a fluid lamellar phase (phase I) [138]. The driving force of the I → II transition, ΔG_{I-II}, implies new energy terms with respect to lamellar-to-lamellar transitions. The most important of these terms is the free energy of bending deformation which has the following form [139,140]:

$$\Delta G_B = 1/2 n_L \times K_c \times A_L (1/R - 1/R_0). \quad (38)$$

In Eq. (38), K_c is the modulus of bending rigidity, R the radius of curvature of the interface (the phospholipid monolayer) delineating the cylinders enclosing internal water and R_0 the radius of intrinsic curvature of this monolayer. This ΔG_B expression refers to a fully hydrated unstressed hexagonal phase for which $R = R_0$ (null bending energy). An additional (unfavorable) free energy term, in the H_{II} phase, is the interstitial energy corresponding to the voids at the junction of the cylinders (Fig. 7C).

The rearrangements of phospholipid and water molecules during a $L_\alpha \rightarrow H_{II}$ transition have been assumed by Siegel and Epand [45] to imply the same intermediates as the fusion process (Section 3.1). Supporting this assumption, the course of this transition is much slower than the main one [141]. This probably arises from the fact that the free energies of these intermediates are higher than those of the initial lamellar phase due to their high curvature (Fig. 7B). Its rate-determining step could be the diffusion of water and phospholipid molecules required for the formation of such intermediates. In order to identify these intermediates, two types of experiments were performed. In the first type (time-resolved X-ray diffraction measurements coupled with T-jumps [116]), an intermediary thin L_α phase, in which ℓ is reduced by 3 Å, has been disclosed. The attribution of this thinning to a reduction of the aqueous interbilayer spaces [123] is supported by a decrease of R_w by 5 when approaching the transition temperature, T_H [142]. In the second type of experiments, time-resolved cryotransmission electron microscopy (TRC-TEM) observations, coupled with pH-jumps [45], have disclosed transient connections between apposed bilayers of multibilayer vesicles. Within clusters of such connections, quasi-hexagonal-like structures have been observed. In contrast to the transient character of these intermediates for most phospholipids, in the case of the diphytanoylphosphatidylcholine, a stable intermediary rhombohedral phase has been identified at a hydration level comprised between those of the L_α and H_{II} phases, in steady-state experiments (Section 3.1, [46,47]). The stability of this intermediate probably arises from the favourable negative intrinsic curvature of this particular phosphatidylcholine.

In either type of experiments, the first step of the $L_\alpha \rightarrow H_{II}$ transition is a mutual approach of apposed bilayers (a dehydration) facilitating local contacts between them (Section 3.1). However, the final volume of internal water is 20–30% larger in the H_{II} phase than in the L_α phase, at T_H [143].

5.3. Isothermal lyotropic transitions

5.3.1. Solvation transitions (implying only the interfacial region)

5.3.1.1. Structural changes (from FT-IR linear dichroism). Structural changes have been observed, at fixed temperature (25 °C), by modifying the hydration level of oriented DODPC multibilayers (a phosphatidylcholine having a rigid diene segment intercalated between the glycerol backbone and each fatty chain), by regulating the RH of the ambient gas phase [144,145]. During dehydration–rehydration scans, in addition to the R_w changes (Fig. 17a), several IR bands, characteristic of phospholipid (Fig. 17b) and associated water (Fig. 18a), exhibit simultaneous changes with hysteresis. Starting from the fully hydrated L_α phase, a dehydration leads to the decrease of $\nu_{as}(CH_2)$ (Fig. 17b) signalling the formation of the $L_{\beta'}$ phase. Hence, an incubation at RH < 0.5 converts this phase into the subgel phase SG_I, the most stable at this hydration level. By rehydration of SG_I, several abrupt modifications occur at RH = 0.6, signalling a new transition ($SG_I \rightarrow SG_{II}$) [145]: R_w jumps (Fig. 17a) and the width of the $\nu_{13}(OH)$ band, $\Delta\nu_{13}(OH)$ jumps (Fig. 18a, right). These jumps reflect the formation of H-bonds between the additionally sorbed water molecules and the PO_2^- headgroup [77]. Besides, the order of fatty chains remains unchanged ($\nu_{as}(CH_2)$ unchanged,

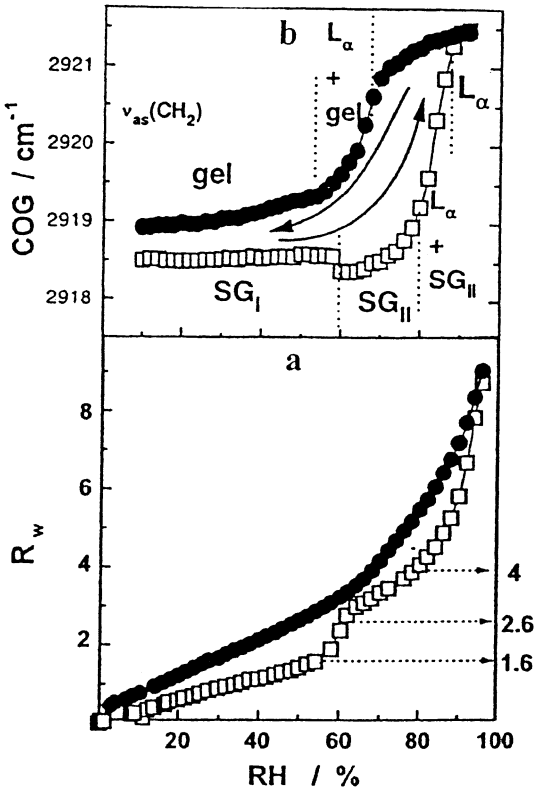

Fig. 17. Hydration/dehydration scans of DODPC/water multibilayers (regulated by the RH, of the ambient gas phase) (reproduced from Ref. [145], with permission). The different symbols correspond to hydration (θ) and dehydration (λ) at 25 °C. The RH ranges corresponding to the different states are indicated by dotted lines. [a] Plot of R_w values as a function of RH. As marked by arrows, a jump of R_w from 1.6 to 2.6 occurs during the $SG_I \rightarrow SG_{II}$ transition. [b] Plot of the wave number of the center of gravity (COG) of the $\nu_{as}(CH_2)$ band of FT-IR spectra as a function of RH. This wave number abruptly changes during the gel ($L_{\beta'}$) → fluid (L_α) and subgel (SG_{II}) → L_α transitions.

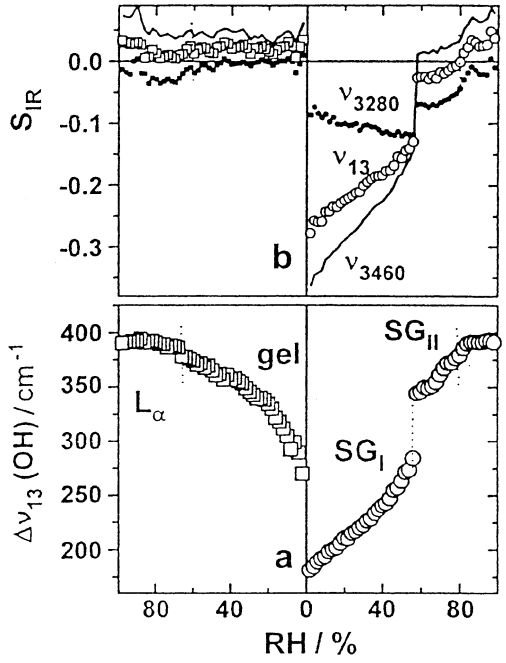

Fig. 18. Action of hydration (right)/dehydration (left) of oriented DODPC/water multibilayers (regulated by the RH of the ambient gas phase), on the features of the ν_{13} water band in their FT-IR spectra (reproduced from Ref. [144], with permission). [a] Plot of its full width at half-maximum (FWHM), $\Delta\nu_{13}$(OH), as a function of RH. This FWHM reflects the broadness of the distribution in strength of H-bonds of interfacial water molecules with the phospholipid headgroups. [b] Plots of the order parameters (S_{IR}) of the orientation of water molecules, at different wave numbers within this band, as a function of RH, deduced from the dichroisms of the corresponding absorbances (see text, Setion 2.3). The low-frequency side of the ν_{13} water band (3280 cm^{-1}) corresponds to a "ν_1-like" stretching mode and its high-frequency side (3460 cm^{-1}) corresponds to a "ν_3-like" stretching mode. The negative values of S_{IR} in the SG_I state indicate that the planes of water molecules are parallel to the membrane interface.

Fig. 17b): the $SG_I \rightarrow SG_{II}$ transition implies only the interfacial region and is called a solvation-induced transition.

Details on the modifications of the interfacial network of H-bonds during these dehydration–rehydration scans are given by the width of the ν_{13}(OH) band, $\Delta\nu_{13}$(OH), and the order parameter, $S_{IR}[\nu_{13}(OH)]$ (Section 2.3). The dehydration-induced gel → SGI transition leads to a drop of $\Delta\nu_{13}$(OH) (Fig. 18a, left) reflecting the reduction of the number of binding sites of water molecules. In the SG_I phase, the negative values of $S_{IR}[\nu_{13}(OH)]$ (Fig. 18b, right) indicate that water molecules are highly ordered (HOH planes of water molecules parallel to the interface). Finally, the rehydration-induced $SG_I \rightarrow SG_{II}$ transition leads to the formation of H-bonds weaker than in the SG_I phase, as reflected by the increase of $\Delta\nu_{13}$(OH) (Fig. 18a, right) and the decrease of $S_{IR}[\nu_{13}(OH)]$ (Fig. 18b, right).

As regards the phosphocholine head as a whole, its orientation is reflected by the order parameters of its phosphate and trimethylammonium headgroups. The modification of these order parameters during the dehydration-induced gel → SG_I transition indicates a rocking of the P^-–N^+ dipoles towards the membrane surface. This rocking agrees with earlier results on the effect of a dehydration [146]. This reorientation of P^-–N^+ dipoles parallels that of water dipoles: they become aligned parallelly to the interface leading to a cancellation of the electrical potentials created by them. This experimental result agrees with simulation results at low hydration (Section 3.2.1, [36,50,51,53]).

These hydration-induced structural changes for lamellar DODPC/water phases can be compared with those of non-lamellar DOPE/water phases [120]. In this latter case, by dehydration, the inverted hexagonal (H_{II}) phase transforms into ribbons characteristic of the P_δ phase [138], by squeezing out of the H_{II} cylinders. This transformation is reflected by modifications of all headgroup vibrational bands. Especially, the occurrence of the $(H_2)N^+$ H. . .OP^-O⇆(H_2)N. . .HOPO proton transfer between the phosphate and ammonium headgroups of adjacent phospholipid molecules is reflected by the narrowness and the splitting of the corresponding bands [79]. By rehydration, a solvation transition ($P_\delta \rightarrow H_{II}$) occurs at RH = 0.6. The modifications of the interfacial region of DOPE/water samples, occurring during the $P_\delta \rightarrow H_{II}$ solvation transition, have been complementarily studied by labelling water (by forming HOD, Section 2.3) [120]. In the dehydrated DOPE P_δ state, the H-bonding of water to discrete binding sites is reflected by a protrusion (at frequencies higher than 3400 cm^{-1}, Fig. 19a, top) of the ν_{13}(OH) band of the uncoupled OH of HOD. By rehydration, during the $P_\delta \rightarrow H_{II}$ transition, the additionally sorbed water molecules bind to both amine and phosphate groups with disappearance of the proton transfer, as reflected by the modifications of the contour of the ν_{13}(OH) band (cf. arrow in Fig. 19a) [79].

5.3.1.2. Energetics of these structural changes (from humidity titration calorimetry). The energetics of the DOPE $P_\delta \rightarrow H_{II}$ and DODPC $SG_I \rightarrow SG_{II}$ solvation transitions has been determined by isothermal humidity titration calorimetry and gravimetric measurements (Section 2.8, [147]). Heat releases, q_{ITC}, and differentials of the sorption isotherms, $\partial(R_w)/\partial(RH)$ corresponding to increments of RH, are represented in Fig. 20a and b by symbols. In the same figures, solid lines represent the integrals of these infinitesimal variations, namely the sorption isotherm, $R_w = f(RH)$, and the integrated heat $Q_{ITC} = f(RH)$. If q_{ITC} corresponds to the variation of enthalpy during the hydration increase, its expression should be the following (Eq. (22), Section 2.8):

$$q_{ITC} = \partial(R_w)/\partial(RH) \times \Delta h'_{hyd} \quad (39)$$

where $\Delta h'_{hyd}$ is the variation of enthalpy during a transfer of one mole of water from the gas to the sorbed phase. Hence, the features of the $Q_{ITC} = f(RH)$ integral should be determined by the slope of the sorption isotherm, $\partial(R_w)/\partial(RH)$. As a confirmation, the $Q_{ITC} = f(RH)$ and $R_w = f(RH)$ plots

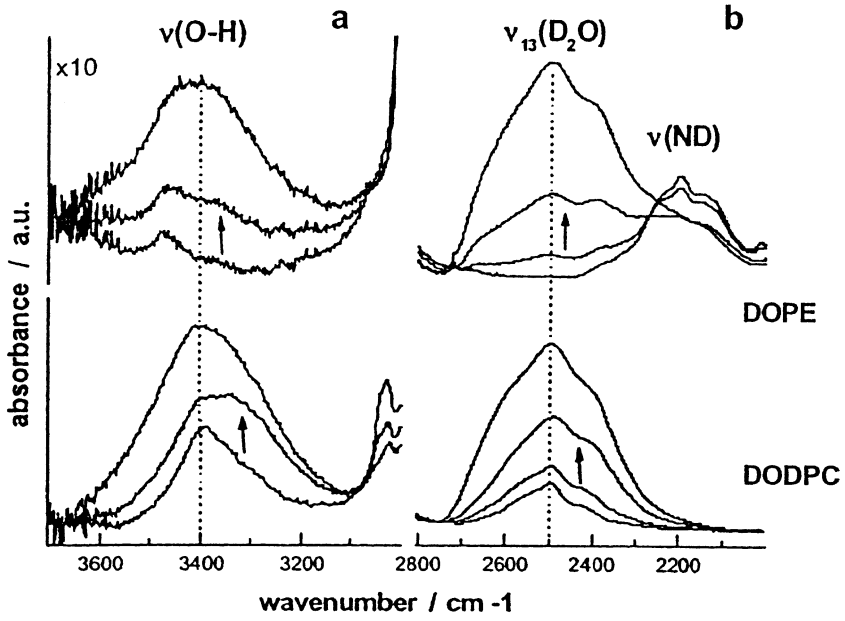

Fig. 19. Action of the hydration of DODPC/water and DOPE/water multibilayers (regulated by the RH of the D_2O/H_2O, 9:1, mol/mol ambient vapour water) on the features of HOD and D_2O water bands (reproduced from Ref. [120] with permission). The contours of these bands, from the bottom to the top, correspond to the following RH values: 0.2, 0.5 (right part only), 0.65 and 0.89. [a] ν(OH) of isolated OH of HOD. [b] ν (OD) of D_2O. The arrows signal the modifications of the contours of these bands occurring during the DOPE $P_\delta \rightarrow H_{II}$ and DODPC $SG_I \rightarrow SG_{II}$ transitions.

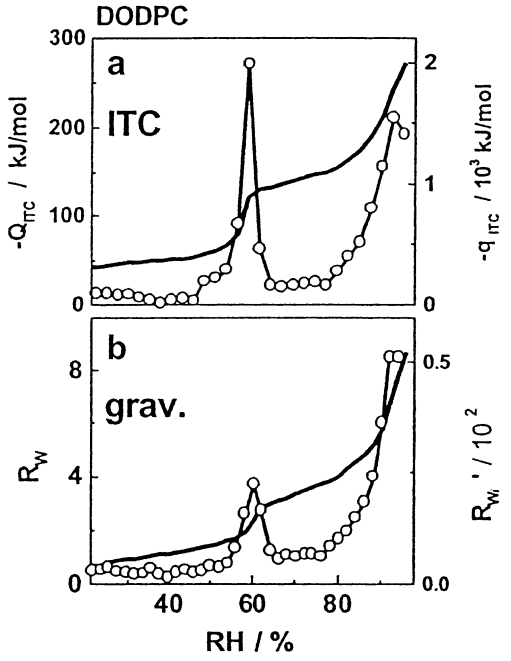

Fig. 20. Influence of increments of the RH of the vapour water above DODPC/water multibilayers, on the slope of their sorption isotherms, $\partial R_w/\partial$RH (b) and on the corresponding heat of water sorption, q_{ITC} (a) (represented by symbols). The integrations of these data are represented by solid lines. They correspond to the functions $Q_{ITC}=f$(RH) (a) and $R_w=f$(RH) (b). These functions exhibit peaks at the same RH value, signalling the $SG_I \rightarrow SG_{II}$ transition. The heats were measured by isothermal titration calorimetry (ITC) and the slopes $\partial R_w/\partial$RH by gravimetry, at 25 °C (reproduced from Ref. [147], with permission).

exhibit peaks at the same RH value (RH = 0.6, Fig. 20a and b). The variations of enthalpy (Δh_{hyd}), entropy (ΔS_{hyd}) and Gibbs free energy (ΔG_{hyd}) corresponding to the DOPE and DODPC transitions, at 25 °C, are reported in Table 1. ΔG_{hyd} values have been obtained from gravimetric measurements (Eq. (20), Section 2.8). They are the same for both DOPE and DODPC transitions ($\Delta G_{hyd} = -1.3$ kJ/mol). Δh_{hyd} values, corresponding to the transfer of liquid water from outside to inside the sample, have been obtained from calorimetric measurements (Section 2.8). As for ΔS_{hyd} values, they have been obtained by difference (Eq. (18)). Finally, for DODPC and DOPE, the Δh_{hyd} values as well as the $T\Delta S_{hyd}$ have opposite signs. The DOPE $P_\delta \rightarrow H_{II}$ tran-

Table 1
Thermodynamical parameters ($\Delta\mu_{hyd}$, Δh_{hyd} and $-T\Delta S_{hyd}$) and changes of the hydration level (ΔR_w), corresponding to the DOPE $P\delta \rightarrow H_{II}$ and the DODPC $SG_I \rightarrow SG_{II}$ transitions (reproduced from [147], with permission)

Lipid phase transition	DOPE $P_\alpha \rightarrow H_{II}$	DODPC $SG_I \rightarrow SG_{II}$
range of R_W	0.5–1.6	1.7 – 2.9
ΔR_W	1.1 ± 0.2	1.2 ± 0.2
a_W	0.60 ± 0.04	0.58 ± 0.4
$\Delta\mu_{hyd}$/kJ/mol	−1.3 ± 0.2	−1.3 ± 0.2
	HTC	HTC
Δh_{hyd}/kJ/mol	13 ± 7	−10 ± 7
$T\Delta S_{hyd}$/kJ/mol	14 ± 7	−9 ± 7

These parameters were deduced from humidity titration calorimetry (HTC) and gravimetric measurements, respectively.

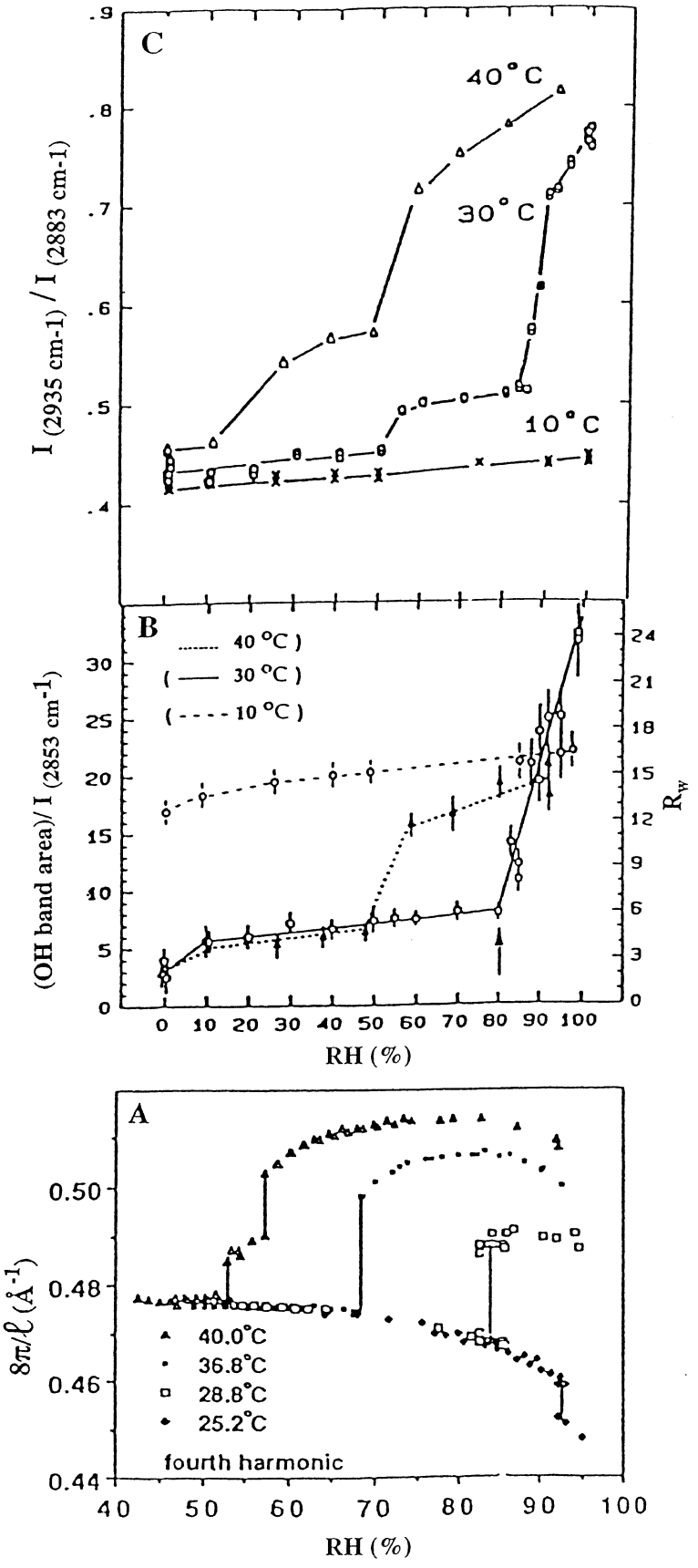
C
40°C
30°C
10°C
I (2935 cm-1) / I (2883 cm-1)
B
40 °C)
30 °C)
10 °C)
(OH band area)/ I (2853 cm-1)
R_W
RH (%)
A
40.0°C
36.8°C
28.8°C
25.2°C
fourth harmonic
$8\pi/\ell$ (Å^{-1})
RH (%)

sition is endothermic and accompanied by an increase of entropy whereas the DODPC $SG_I \rightarrow SG_{II}$ transition is exothermic and accompanied by a decrease of entropy. These different energetic characteristics arise from the difference of the structural transformations occurring in the interfacial network of H-bonds. During the DOPE $P_\delta \rightarrow H_{II}$ transition, the proton transfer between phosphate and amine headgroups of two adjacent phospholipid molecules is broken down resulting in a disordering of the interfacial region. This leads to an unfavourable endothermicity and a gain in entropy. In contrast, during the DODPC $SG_I \rightarrow SG_{II}$ transition, the additionally sorbed water molecules form strong H-bonds with headgroups. This leads to a favourable exothermicity and a gain in order (an unfavorable loss of entropy). Thus, during a phospholipid hydration, according to the nature and the strength of the H-bonds formed and broken down, either a favourable variation of enthalpy or a favourable variation of entropy can result. This interchangeability between enthalpy and entropy, during hydration processes, is a universal phenomenon due to the capability of water to reorganize its H-bond network [148].

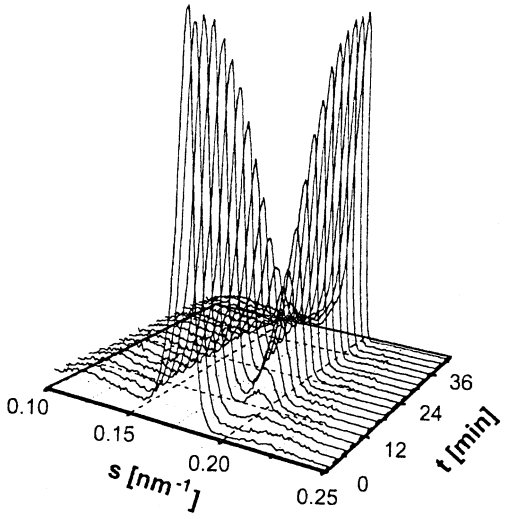

Fig. 22. Time-resolved small-angle X-ray scattering patterns of POPC/water multibilayers obtained during a hydration scan (regulated by the RH of the ambient gas phase) at 26 °C (reproduced from Ref. [151], with permission). The first-order Bragg reflection corresponding to the hydrated L_α phase gradually rises at the expense of that corresponding to the dry L_β phase.

5.3.2. Chain-disordering lyotropic transitions

Chain-disordering lyotropic transitions can be triggered by changes of the RH of the ambient gas phase at fixed temperature, as disclosed by two types of experiments on DMPC/water samples. First, Raman scattering measurements were performed [149]. Using as marker of the degree of order of fatty chains the ratio of the intensities, $I_{2935cm} - 1/I_{2883cm} - 1$, in the spectra, drops of this ratio (signalling orderings of fatty chains) have been observed by dehydration, at RH = 0.55 at 40 °C, and RH = 0.86 at 30 °C (Fig. 21C). Second, X-ray diffraction measurements were performed [26]. Jumps of ℓ at RH = 0.57 at 40 °C, and at RH = 0.84 at 30 °C (signalling straigthenings of fatty chains), have been disclosed (Fig. 21A). In addition, the integrated intensity of the O–H stretching band in Raman spectra has been found to exhibit discontinuities at $0.5 \leq RH \leq 0.6$ at 40 °C, and at RH = 0.8 at 30 °C (Fig. 21B, [149]). All these results reflect dehydration-induced fluid (L_α) → gel (L'_β) DMPC transitions. Such osmotic-stress-induced main transitions have been recently confirmed by two groups of authors. First, Markova et al. [5] have observed with their double-twin calorimeter that the inverse gel (L'_β) → fluid (L_α) transition occurs at RH ~ 0.9 at 27 °C. Second, Hung et al. [150] have observed, by osmotic stress of DMPC films, a jump of the ℓ values at $\pi_{osm} \sim 2.5 \times 10^7$ Pa at 30 °C.

The mechanism of a lyotropic chain-disordering transition is revealed by more sophisticated experiments [151]; the response of POPC to a RH-controlled hydration at room temperature has shed light on this. First, the electron density profiles of POPC/water multibilayers have been obtained by a near-equilibrium X-ray diffraction study as a function of RH [142]. Decomposing in submolecular fragments, similarly to the White and Wiener's method [13], the positions along the bilayer normal of these fragments can be calculated. Upon increasing RH, these positions abruptly change at around RH = 0.4, signalling a direct $L_\beta \rightarrow L_\alpha$ transition. From these changes of positions of fragments, the variations of the thicknesses of the phospholipid and water layers can be inferred: ℓ decreases by 6 Å while ℓ_w stays approximatively constant. It can be concluded that phospholipid bilayers contract vertically and expand laterally (volume of the bilayer incompressible). As the relative variation of ℓ_L is 10%, A_L should increase by 10%. This lateral expansion has been confirmed by more recent humidity-controlled X-ray diffraction measurements [75]: A_L has been found to increase by 14% at RH = 0.4 (Fig. 10-(2)). From this increase in area, the transbilayer flux of water, triggered by the transbilayer gradient of water chemical potential, is amplified (Section 4.3). From then on, water molecules flowing around fatty chains lead to their disordering (interdependence of the

Fig. 21. Action of the RH of the vapour phase, hydrating a DMPC/water multibilayer sample, on its lamellar repeat period, ℓ, and its Raman spectra (reproduced from Refs. [26,149], respectively). (A) Plots of $8\pi/\ell$ spacing values of a freely suspended DMPC film, measured by X-ray diffraction, as a function of RH. These plots exhibit discontinuities at RH = 58% at 40 °C, RH = 84% at 28.8 °C and RH = 68% at 36.8 °C. (C) Plots of the ratio of light intensities, after Raman diffusion, at two wave numbers (2935 and 2883 cm^{-1}), within the CH_2 stretching band, as a function of RH. This ratio is used as a marker of the degree of order of fatty chains. These plots exhibit discontinuities at RH = 55% and 20% at 40 °C and at RH = 86% and 52% at 30 °C. (B) Plots of the integrated intensities of the OH band of the Raman spectra (normalized with respect to the intensity at 2853 cm^{-1}) as a function of RH. These intensities are converted in R_w values (right-hand scale). These plots exhibit discontinuities at: (i) RH ~ 85% at 30 °C (where R_w is reduced by 19); (ii) RH = 50–60% at 40 °C (where R_w is reduced by 6). All these discontinuities signal phase transitions.

chemical potentials of phospholipid and water; Section 2.7, Eq. (16)). Such a mechanism has been confirmed by a recent study of the dynamics of the RH-controlled $L_\beta \rightarrow L_\alpha$ transition by time-resolved X-ray diffraction [151]. As shown in Fig. 22, upon increasing RH from 0% to 100%, the intensity of the Bragg reflection corresponding to the hydrated L_α phase gradually increases at the expense of that corresponding to the "dry" L_β phase. This process lasts several minutes. The slowness of this transition, compared to a thermal transition (a few seconds, [132]), is highly relevant. It reflects the slowness of the regulation of the transformation by the influx of water through the multibilayer stack up to equilibration of the water chemical potentials inside and outside (vapour) the sample (represented respectively by compartments II and I in Fig. 2).

6. Conclusion

All the results discussed above (Section 5) lead to the conclusion that each thermodynamical phase of model membranes is characterized by a specific hydration level and a specific distribution of water molecules. Quantitatively, the hydration state is defined by the number of water molecules trapped in the interbilayer spaces of phospholipid/water multibilayers (denoted by R_w). Qualitatively, it is defined by the properties of this water (Section 3.2), recalled below. First, the thermodynamical state of interbilayer water molecules (their space-averaged chemical potential) and, thereby, their freezing temperature change during phase transitions. For instance, the subtransition occurs for a specific state of interbilayer water (Fig. 16, [59,62]). Whether it is the cause or the consequence of this transition is difficult to discern. Second, the degree of order of the orientation of the electric dipoles of water molecule abruptly changes at the main phase transition (as reflected by the ^{2}H-NMR spectra shown in Fig. 12, [94]). Third, the dynamics of this orientation depends on the confinement of water molecules either within the interbilayer spaces of phospholipid/water multibilayers or within the core of phospholipid-based reverse micelles. This dependence is reflected by the effect of two types of electric fields. On the one hand, that resulting from the displacement of charges borne by phospholipid headgroups (triggered, for instance, by an alternating electric field, Section 2.6). These motions induce a dielectric relaxation of surrounding water molecules whose frequency depends on the narrowness of the interbilayer spaces of a phospholipid/water multibilayer (its hydration level; Section 3.5, [152]). On the other hand, the electric field, due to the displacement of electrons of a fluorescent molecule by excitation, induces a reorientation of surrounding water molecules. If this molecule is dissolved in the water core of reverse micelles, the rapidity of this reorientation depends on the size of this core, i.e. the R_w value (Section 3.6, [66]). In both cases, the orientational mobility of water molecules depends on the disposable volume (i.e. on the hydration level). It is the confinement which slows down water molecules rather than their H-bonding with headgroups (Sections 3.2.4 and 3.6). Generally speaking, phospholipid-sorbed water is composed of differently H-bonded populations of molecules in permanent exchange. These populations can be distinguished when their exchange is slow compared to the time window of the observation method. On the time window of ^{2}H-NMR (10^{-5} s), this exchange is fast in the case of a fully hydrated fluid lamellar phase, and only one ^{2}H-NMR spectrum is observed (in absence of phase transition). On the time window of DSC ($\sim 1°$/min), at the temperature range corresponding to the subgel phase, this exchange is sufficiently slow so that different populations of water molecules can be distinguished according to their freezing temperatures (Section 5.2.2).

In order to better understand this interdependence of the states of phospholipid and sorbed water, it is necessary to come back at the origin of the hydration. The activity of the phospholipid-sorbed water is governed by that of water of the hydration source (Fig. 2). When an equilibrium is established between the phospholipid sample and this source, the two variables which fully define the final state of the sample (at fixed pressure) are temperature and water activity. This activity, in case of the new humidity-controlled osmotic stress experiments (Section 2.7), is equal to the RH of the ambient vapour phase (Fig. 2, $a^I = a^{II} = RH$). More generally, this activity of water (and, thereby, its chemical potential) is an intensive parameter of the thermodynamical state of phospholipid /water two-component systems. These systems are at equilibrium when, everywhere in it, this parameter is uniform. In other terms, any heterogeneity of the water chemical potential entails a displacement of water molecules: a transmembrane gradient of the water chemical potential automatically generates a transmembrane flux of water (Section 2.7, Eq. (11), Fig. 3). Hence, the ebb and flow of these internal water molecules modulate the conformation of the fatty chains (the chemical potential of the phospholipid molecule), due to the interdependence of the chemical potentials of phospholipid and sorbed water molecules (Gibbs–Duhem relation, Eq. (16)). Therefore, phase transitions can be triggered either at a specific value of the water activity (of RH) at fixed temperature (lyotropic transitions) or at a specific temperature at fixed activity (thermal transitions).

During the thermal transitions, the first rapid step is the creation of defects in the chain packing of phospholipid bilayers (melting of chains in isolated phospholipid molecules). Such defects appear as soon as a few degrees below T_m [132,133]. Subsequently, in a less rapid step, rearrangements, like the gathering of phospholipid molecules with molten chains in domains, occur. These rearrangements can lead, for instance, to the periodic ripples characteristic of the rippled (P'_β) phase [129]. They would be very slow if proceeding only by diffusion of phospholipid molecules.

In fact, they proceed mainly by *redistribution of more mobile water molecules*, as evidenced by time-resolved X-ray diffraction measurements [132].

During lyotropic transitions, transformations similar to those occurring during thermal transitions occur. These transformations imply either the interfacial region only (solvation transitions, Section 5.3.1) or also the hydrocarbon region (Section 5.3.2). They have been identified by different methods (isothermal titration calorimetry, Section 5.3.1.2, [147]; X-ray scattering, Section 5.3.2, [26,151]; FT-IR linear dichroism, Section 5.3.1.1, [144,145]). Concerning lyotropic chain-disordering (ordering) transitions, the mechanism can appear obscure. Of course, increasing hydration leads to a swelling of the polar heads, easing up isomerizations of fatty chains. However, this is not sufficient to overcome the energy barrier opposed to such isomerizations. We think that these transitions, like the solvation transitions, imply chemical contacts between water and phospholipid molecules. As a matter of fact, the presence of water molecules within the hydrocarbon region of phospholipid bilayers is feasible owing to the interconnection of free-volumes present in this region (Section 4.3, [112]) and has been detected in fluid model membranes from fluorescence experiments (Section 4.2, [105]). During an osmotic stress, the transmembrane flux of water generated by the transmembrane gradient of the water chemical potential is amplified (or restrained) by the change of the water-activity-dependent cross-sectional area per phospholipid molecule (Sections 4.3 and 5.3.2, Fig. 10-(2), [75]) which accelerates the change of order of fatty chains.

Generally speaking, the capability of water of playing the role of an energy transducer has been revealed, for instance, by the thermodynamical characteristics of the hydration of apolar compounds. The corresponding variation of the Gibbs free energy is quasi-insensitive to the temperature. This results from opposite temperature dependences of the enthalpy and entropy terms (enthalpy–entropy compensation, Ref. [148] and references herein) of this free energy. We have seen an example of this compensation in the characteristics of the energetics of DODPC $SG_I \rightarrow SG_{II}$ and DOPE $P_\delta \rightarrow H_{II}$ transitions (Section 5.3.1.2) which differ. This enthalpy–entropy compensation results from particular properties of liquid water [148]. Different models of liquid water were devised for interpreting it. Coarsely, these models consider water as a mixture of free and hydration water. In these two states, number, strength and orientational order of H-bonds are different. Owing to the balance between free and hydration water and the consequential organization of the H-bond network, entropic and enthalpic terms of the variation of the Gibbs free energy during the introduction of a solute in liquid water can compensate one another. Indeed, we have seen that water present in the hydrocarbon region of phospholipid bilayers is organized in single files of H-bonded molecules (Sections 3.2.1 and 4.3, [49]): the arrangement and, thereby, the chemical potential of water molecules depend on their environment. Conversely, within this environment, the conformation of phospholipid molecules (their chemical potential) is modified by interaction with surrounding water molecules. The general thermodynamic explanation of this interplay between water molecules and their environment has been given by Parsegian, Rand and Rau [1,153]. More generally, within a cell, water at the surface of the biological macromolecules propagates energy and, thereby, plays the role of a ubiquitous heterogeneous interface [154].

The perspectives open by these results are immense. Indeed, if the chemical potential of water molecules enclosed in the smallest free-volumes of the interfacial and hydrocarbon regions of membranes regulates their thermodynamical state, this can in turn greatly affect the activity of membranous proteins (Ref. [155] and references herein). Such perspectives are strong incentives and we hope that experiments and simulations will soon be devoted to these issues.

Acknowledgements

The author thanks Dr. Pascale Mentré and Dr. Jacques Bolard for their critical reading of her manuscript. She especially thanks Dr. Lisbeth Terminassian-Saraga for her pieces of competent advice. She also thanks authors who have kindly authorized her to reproduce their figures.

References

[1] V.A. Parsegian, R.P. Rand, D.C. Rau, Macromolecules and water: probing with osmotic stress, Methods Enzymol. 259 (1995) 43–94.
[2] Hydration processes in biological and macromolecular systems, Faraday Discuss. 103 (1996).
[3] R.P. Rand, V.A. Parsegian, Hydration forces between phospholipid bilayers, Biochim. Biophys. Acta 988 (1989) 351–376.
[4] H. Binder, B. Kohlstrunk, H.H. Heerklotz, Hydration and lyotropic melting of amphiphilic molecules: a thermodynamic study using humidity titration calorimetry, J. Colloid Interface Sci. 220 (1999) 235–249.
[5] N. Markova, E. Sparr, L. Wadsö, H. Wennerström, A calorimetry study of phospholipid hydration. Simultaneous monitoring of enthalpy and free energy, J. Phys. Chem., B 104 (2000) 8053–8060.
[6] F. Volke, S. Eisenblätter, G. Klose, Hydration force parameters of phosphatidylcholine lipid bilayers as determined from ^{2}H-NMR studies of deuterated water, Biophys. J. 67 (1994) 1882–1887.
[7] A.S. Ulrich, A. Watts, Lipid headgroup hydration studied by ^{2}H-NMR: a link between spectroscopy and thermodynamics, Biophys. Chem. 49 (1994) 39–50.
[8] W. Pohle, C. Selle, H. Fritzsche, H. Binder, FT-IR spectroscopy as a probe for the study of the hydration of lipid self-assemblies. I: Methodology and general phenomena, Biospectroscopy 4 (1998) 267–280.
[9] D.P. Teleman, S.J. Marrink, H.J. Berendsen, A computer perspective of membranes: molecular dynamics studies of lipid bilayer systems, Biochim. Biophys. Acta 1331 (1997) 235–270.
[10] M. Bloom, E. Evans, O.G. Mouritsen, Physical properties of the fluid lipid-bilayer component of cell membranes: a perspective, Q. Rev. Biophys. 24 (1991) 293–397.
[11] T.J. McIntosh, X-ray Diffraction Analysis of Membrane Lipids, in: R. Brasseur (Ed.), Molecular Description of Biological Membranes

by Computer-Aided Conformational Analysis, vol. I, CRC Press, 1990, pp. 247–265.
[12] T.J. McIntosh, S.A. Simon, Area per molecule and distribution of water in fully hydrated dilauroylphosphatidylethanolamine bilayers, Biochemistry 25 (1986) 4948–4952.
[13] S.H. White, M.C. Wiener, Determination of the structure of lipid bilayers, in: E.A. Disalvo, S.A. Simon (Eds.), Permeability and Stability of Lipid Bilayers, CRC Press, 1995, pp. 1–19.
[14] H.I. Petrache, N. Gouliaev, S. Tristram-Nagle, R. Zhang, R.M. Suter, J.F. Nagle, Interbilayer interactions from high-resolution X-ray scattering, Phys. Rev., E 57 (1998) 7014–7024.
[15] J.F. Nagle, S. Tristram-Nagle, Structure of lipid bilayers, Biochim. Biophys. Acta 1469 (2000) 159–195.
[16] R.L. Thurmond, G. Lindblom, NMR studies of membrane lipid properties, Curr. Top. Membr., Acad. Press, 1997, Chap. 3.
[17] J. Seelig, A. Seelig, Lipid conformation in model membranes and biological membranes, Q. Rev. Biophys. 13 (1980) 19–61.
[18] E. Goormaghtigh, J.M. Ruysschaert, Polarized attenuated total reflection infrared spectroscopy as a tool to investigate the conformation and orientation of membrane components, in: R. Brasseur (Ed.), Molecular Description of Biological Membranes by Computer Aided Conformational Analysis, 1990, pp. 285–329.
[19] H. Binder, The molecular architecture of lipid membranes. New insights from hydration-tuning infrared linear dichroism spectroscopy, Appl. Spectrosc. Rev. 38 (2003) 15–69.
[20] A. Chattopadhyay, Exploring membrane organization and dynamics by the wavelength-selective fluorescence approach, Chem. Phys. Lipids 122 (2003) 3–17.
[21] S. KumarPal, J. Peon, B. Bagchi, A.H. Zewail, Biological water: femtosecond dynamics of macromolecular hydration, J. Phys. Chem., B 106 (2002) 12376–12395.
[22] J.R. Lacowicz, Principles of Fluorescence Spectroscopy, Kluwer Academic/Plenum Publishers, 1999.
[23] A. Blume, Applications of Calorimetry to Lipid Model Membranes, in: C. Hidalgo (Ed.), Physical Properties of Biological Membranes and their Applications, 1988, pp. 71–121.
[24] U. Kaatze, A. Dittrich, K.D. Göpel, R. Pottel, Dielectric studies on water in solutions of purified lecithin vesicles, Chem. Phys. Lipids 35 (1984) 279–290.
[25] M.H. Friedman, Principles and Models of Biological Transport, Springer-Verlag, Berlin, 1986.
[26] G.S. Smith, C.R. Safinya, R.J. Plano, N.A. Clark, X-ray structural studies of freely suspended ordered hydrated DMPC multimembrane films, J. Chem. Phys. 92 (1990) 4519–4529.
[27] G. Klose, B. König, F. Paltauf, Sorption isotherms and swelling of POPC in H_2O and ^2H_2O, Chem. Phys. Lipids 61 (1992) 265–270.
[28] N. Markova, E. Sparr, L. Wadsö, On application of an isothermal sorption microcalorimeter, Thermochim. Acta 374 (2001) 93–104.
[29] T.J. McIntosh, A.D. Magid, Phospholipid hydration, in: G. Cevc (Ed.), Phospholipids Handbook, Marcel Dekker, 1993, pp. 553–577.
[30] E. Tüchsen, M.O. Jensen, P. Wesh, Solvent accessible surface area (ASA) of simulated phospholipid membranes, Chem. Phys. Lipids 123 (2003) 107–116.
[31] D.F. Evans, H. Wennerström, The Colloidal Domain: Where Physics, Chemistry, Biology and Technology Meet, Wiley, 1998.
[32] T.J. McIntosh, Hydration properties of lamellar and non-lamellar phases of phosphatidylcholine and phosphatidylethanolamine, Chem. Phys. Lipids 81 (1996) 117–131.
[33] D.M. LeNeveu, R.P. Rand, V.A. Parsegian, D. Gingell, Measurement and modification of forces between lecithin bilayers, Biophys. J. 18 (1977) 203–209.
[34] J. Israelachvili, H. Wennerström, Role of hydration and water structure in biological and colloidal interactions, Nature 379 (1996) 219–225.
[35] V.A. Parsegian, R.P. Rand, On molecular protrusion as the source of hydration forces, Langmuir 7 (1991) 1299–1301.
[36] S.J. Marrink, M. Berkowitz, H.J.C. Berendsen, Molecular dynamics simulation of a membrane/water interface: the ordering of water and its relation to the hydration force, Langmuir 9 (1993) 3122–3131.
[37] H. Binder, U. Dietrich, M. Schalke, H. Pfeiffer, Hydration-induced deformation of lipid aggregates before and after polymerization, Langmuir 15 (1999) 4857–4866.
[38] T. McIntosh, Short-range interactions between lipid bilayers measured by XR diffraction, Curr. Opin. Struct. Biol. 10 (2000) 481–485.
[39] T. Honger, K. Mortensen, J.H. Ipsen, J. Lemmich, R. Bauer, O.G. Mouristen, Anomalous swelling of multilamellar lipid bilayers in the transition region by renormalization of curvature elasticity, Phys. Rev. Lett. 72 (1994) 3911–3914.
[40] L. Chernomordik, M.M. Kozlov, J. Zimmerberg, Lipids in biological membrane fusion, J. Membr. Biol. 146 (1995) 1–14.
[41] R. Jahn, H. Grubmüller, Membrane fusion, Curr. Opin. Cell Biol. 14 (2002) 488–495.
[42] L.V. Chernomordik, G.B. Melikyan, Y.A. Chizmadzhev, Biochim. Biophys. Acta 906 (1987) 309–352.
[43] G. Lei, R.C. MacDonald, Lipid bilayer vesicle fusion: intermediates captured by high-speed microfluorescence spectroscopy, Biophys. J. 85 (2003) 1585–1599.
[44] D.P. Siegel, The modified stalk mechanism of lamellar/inverted phase transitions and its implications for membrane fusion, Biophys. J. 76 (1999) 291–313.
[45] D.P. Siegel, R.M. Epand, The mechanism of lamellar-to-inverted hexagonal phase transitions in phosphatidylethanolamine: implications for membrane fusion mechanisms, Biophys. J. 73 (1997) 3089–3111.
[46] L. Yang, H.W. Huang, Observation of a membrane fusion intermediate structure, Science 297 (2002) 1877–1879.
[47] L. Yang, H.W. Huang, A rhombohedral phase of lipid containing a membrane fusion intermediate structure, Biophys. J. 84 (2003) 1808–1817.
[48] L. Yang, T.M. Weiss, R.I. Lehrer, H.W. Huang, Crystallization of antimicrobial pores in membranes magainin and protegrin, Biophys. J. 79 (2000) 2002–2009.
[49] S.J. Marrink, H.J.C. Berendsen, Simulation of water transport through a lipid membrane, J. Phys. Chem. 98 (1994) 4155–4168.
[50] P. Jedlovsky, M. Mezei, Orientational order of the water molecules across a fully hydrated DMPC bilayer: a Monte Carlo simulation study, J. Phys. Chem., B 105 (2001) 3614–3623.
[51] F. Zhou, K. Schulten, Molecular dynamics study of a membrane–water interface, J. Phys. Chem., B 99 (1995) 2194–2207.
[52] K. Gawrisch, D. Ruston, J. Zimmerberg, V.A. Parsegian, R.P. Rand, N. Fuller, Membrane dipole potential, hydration forces, and the ordering of water at membrane surfaces, Biophys. J. 61 (1992) 1213–1223.
[53] R.J. Mashl, H.L. Scott, S. Subramaniam, E. Jakobsson, Molecular simulation of dioleoylphosphatidylcholine lipid bilayers at different levels of hydration, Biophys. J. 81 (2001) 3005–3015.
[54] J.F. Nagle, M.C. Wiener, Structure of fully hydrated bilayer dispersions, Biochim. Biophys. Acta 942 (1988) 1–10.
[55] O. Narayan, P.T.C. So, D.C. Turner, S.M. Gruner, M.W. Tate, E. Shyamsunder, Volume constriction in a lipid–water liquid crystal using high-pressure X-ray diffraction, Phys. Rev., A 42 (1990) 7479–7482.
[56] J.T. Gleeson, S. Erramilli, S.M. Gruner, Freezing and melting water in lamellar structures, Biophys. J. 67 (1994) 706–712.
[57] L. Terminassian-Saraga, G. Madelmont, Differential scanning calorimetry studies of hydration forces with phospholipid multilamellar systems, J. Colloid Interface Sci. 85 (1982) 375–388.
[58] C. Grabielle-Madelmont, R. Perron, Calorimetric studies on phospholipid–water studies II Study of water behavior, J. Colloid Interface Sci. 95 (1983) 483–493.

[59] M. Kodama, H. Hashigami, S. Seti, Role of water molecules in the subtransition of the L-DPPC–water system as studied by DSC, J. Colloid Interface Sci. 117 (1987) 497–504.
[60] V.L. Bronshteyn, P.L. Steponkus, Calorimetric studies of freeze-induced dehydration of phospholipids, Biophys. J. 65 (1993) 1853–1865.
[61] A.S. Ulrich, M. Sami, A. Watts, Hydration of DOPC bilayers by DSC, Biochim. Biophys. Acta 1991 (1994) 225–230.
[62] M. Kodama, H. Inoue, Y. Tsuchida, The behavior of water molecules associated with structural changes in phosphatidylethanolamine assembly as studied by DSC, Thermochim. Acta 266 (1995) 373–384.
[63] M. Lafleur, M. Pigeon, M. Pézolet, J.P. Caillé, Raman spectrum of interstitial water in biological systems, J. Phys. Chem. 93 (1989) 1522–1526.
[64] N. Nandi, B. Bagchi, Dielectric relaxation of biological water, J. Phys. Chem., B 101 (1997) 10954–10961.
[65] A.S. Ulrich, A. Watts, Molecular response of the lipid headgroup to bilayer hydration monitored by ^{2}H-NMR, Biophys. J. 66 (1994) 1441–1449.
[66] D.M. Willard, R.E. Riter, N.E. Levinger, Dynamics of polar solvation in lecithin/water/cyclohexane reverse micelles, J. Am. Chem. Soc. 120 (1998) 4151–4160.
[67] A. Scodinu, J.T. Fourkas, Comparison of the orientational dynamics of water confined in hydrophobic and hydrophilic nanopores, J. Phys. Chem., B 106 (2002) 10292–10295.
[68] G. Klose, B. König, H.W. Meyer, G. Schulze, G. Degovics, Small-angle X-ray scattering and electron-microscopy of crude dispersions of swelling lipids and the influence of the morphology on the repeat distance, Chem. Phys. Lipids 47 (1988) 225–234.
[69] S.C. Costigan, P.J. Booth, R.H. Templer, Estimations of lipid bilayer geometry in fluid lamellar phases, Biochim. Biophys. Acta 1468 (2000) 41–54.
[70] J.R. Scherer, On the position of the hydrophobic/hydrophilic boundary in lipid bilayers, Biophys. J. 55 (1989) 957–964.
[71] N. Boden, S.A. Jones, F. Sixl, On the use of deuterium nuclear magnetic resonance as a probe of chain packing in lipid bilayers, Biochemistry 30 (1991) 2146–2155.
[72] T. LeBihan, M. Pézolet, Study of the structure and phase behavior of dipalmitoylphosphatidylcholine by infrared spoectroscopy: characterization of the pretransition and subtransition, Chem. Phys. Lipids 94 (1998) 13–33.
[73] V.R. Kodati, M. Lafleur, Comparison between orientational and conformational orders in fluid lipid bilayers, Biophys. J. 64 (1993) 163–170.
[74] B.W. Koenig, H.H. Strey, K. Gawrisch, Membrane lateral compressibility determined by NMR and X-ray diffraction: effect of acyl chain polyunsaturation, Biophys. J. 73 (1997) 1954–1966.
[75] H. Binder, K. Gawrisch, Dehydration induces lateral expansion of polyunsaturated 18:0-22:6 phosphatidylcholine in a new lamellar phase, Biophys. J. 81 (2001) 969–982.
[76] P.T.T. Wong, H.H. Mantsch, High-pressure IR spectroscopic evidence of water binding sites in 1, 2-diacyl phospholipids, Chem. Phys. Lipids 46 (1988) 213–224.
[77] J. Grdadolnik, J. Kidric, D. Hadzi, Hydration of phosphatidylcholine reverse micelles and multilayers. An IR study, Chem. Phys. Lipids 59 (1991) 57–68.
[78] A. Blume, W. Hübner, G. Messner, Fourier transform infrared spectroscopy of 13C=O-labeled phospholipids. Hydrogen bonding to carbonyl groups, Biochemistry 27 (1988) 8239–8249.
[79] R.N.A. Lewis, R.N. McElhaney, Calorimetric and spectroscopic studies of the polymorphic phase behavior of a homologous series of n-saturated 1, 2-diacylphosphatidylethanolamines, Biophys. J. 64 (1993) 1081–1096.
[80] K.V. Damodaran, K.M. Merz Jr., Headgroup–water interactions in lipid bilayers: a comparison between DMPC- and DLPE-based lipid bilayers, Langmuir 9 (1993) 1179–1183.
[81] K.V. Damodaran, K.M. Merz Jr., A comparison of DMPC- and DLPE-based lipid bilayers, Biophys. J. 66 (1994) 1076–1087.
[82] L. Perera, U. Essman, M.L. Berkowitz, The role of water in the hydration force-molecular dynamics simulations, Prog. Colloid & Polym. Sci. 103 (1997) 107–115.
[83] T.J. McIntosh, S.A. Simon, Adhesion between phosphatidylethanolamine bilayers, Langmuir 12 (1996) 1622–1630.
[84] M. Pasenkiewcz-Gierula, Y. Takaoka, H. Miyagawa, K. Kitamur, A. Kusumi, Hydrogen bonding of water to phosphatidylcholine in the membrane as studied by a molecular dynamics simulation: location, geometry, and lipid–lipid bridging via hydrogen-bonded water, J. Phys. Chem., A 101 (1997) 3677–3691.
[85] M. Pasenkiewicz-Gierula, Y. Takaoka, H. Miyagawa, K. Kitamura, A. Kusumi, Charge pairing of headgroups in phosphatidylcholine membranes: a molecular dynamics simulation study, Biophys. J. 76 (1999) 1228–1240.
[86] H. Morgan, D.M. Taylor, O.N. Oliveira Jr., Two-dimensional proton conduction at a membrane surface: influence of molecular packing and hydrogen-bonding, Chem. Phys. Lett. 150 (1988) 311–314.
[87] J. Teissié, M. Prats, P. Soucaille, J.F. Tocanne, Evidence for conduction of protons along the interface between water and polar lipid monolayers, Proc. Natl. Acad. Sci. U. S. A. 82 (1985) 3217–3221.
[88] J. Heberle, J. Riesle, G. Thiedemann, D. Oesterhelt, N.A. Dencher, Proton migration along the membrane surface and retarded surface to bulk transfer, Nature 370 (1994) 379–382.
[89] J. Zhang, P.R. Unwin, Proton diffusion at phospholipid assemblies, J. Am. Chem. Soc. 124 (2002) 2379–2383.
[90] Proton Transfer Reactions in Bioenergetics, Biochim. Biophys. Acta 1458 (2000).
[91] S. Bratos, H. Ratajczac, P. Viot, Properties of H-bonding in the infrared spectral range, in: J.C. Dore, J. Teixera (Eds.), H-bonded Liquids, Kluwer Academic Publishing, 1991, pp. 221–235.
[92] F. Volke, S. Eisenblatter, J. Galle, G. Klose, Dynamic properties of water at phosphatidylcholine lipid bilayer surfaces as seen by deuterium and pulsed field gradient ^{1}H-NMR, Chem. Phys. Lipids 70 (1994) 121–132.
[93] S.R. Wassal, PFGSE-NMR studies of water diffusion in a phospholipid model membrane, Biophys. J. 71 (1996) 2724–2732.
[94] S. König, E. Sackmann, D. Richter, R. Zorn, C. Carlile, T.M. Bayerl, Molecular dynamics of water in oriented DPPC multilayers studied by quasielastic neutron scattering and deuterium-nuclear magnetic resonance relaxation, J. Chem. Phys. 100 (1994) 3307–3316.
[95] J.C.W. Shepherd, G. Büldt, Zwitterionic dipoles as a dielectric probe for investigating head group mobility in phospholipid membranes, Biochim. Biophys. Acta 514 (1978) 83–94.
[96] G. Nimtz, A. Enders, B. Binggeli, Hydration dependence of the head group mobility in phospholipid (DMPC) membranes, Ber. Bunsenges, Phys. Chem. 89 (1985) 842–845.
[97] C.H. Hsieh, W. Wu, Structure and dynamics of primary hydration shell of phosphatidylcholine bilayers at subzero temperatures, Biophys. J. 71 (1996) 3278–3287.
[98] C.H. Hsieh, W. Wu, Three distinct types of unfrozen water in fully hydrated phospholipid bilayers: a combined ^{2}H- and ^{31}P-NMR study, Chem. Phys. Lipids 78 (1995) 37–45.
[99] K. Bhattacharyya, B. Bagchi, Slow dynamics of constrained water in complex geometries, J. Phys. Chem., A 104 (2000) 10603–10613.
[100] R.S. Armen, O.D. Uitto, S.E. Feller, Phospholipid component volumes: determination from bilayer structural calculations, Biophys. J. 75 (1998) 734–744.
[101] S.E. Feller, D. Yin, R.W. Pastor, A.D. McKerell Jr., Molecular dynamics simulation of unsaturated lipid bilayers at low hydration: parameterization and comparison with diffraction studies, Biophys. J. 73 (1997) 2269–2279.
[102] S.E. Feller, R.M. Venable, R.W. Pastor, Computer simulation of a DPPC phospholipid bilayer: structural changes as a function of molecular surface area, Langmuir 13 (1997) 6555–6561.

[103] H.I. Petrache, S.E. Feller, J.F. Nagle, Determination of component volumes of lipid bilayers from simulations, Biophys. J. 72 (1997) 2237–2242.
[104] E. Perochon, A. Lopez, J.F. Tocanne, Polarity of lipid bilayers. A fluorescence investigation, Biochemistry 31 (1992) 7672–7682.
[105] A. Chattopadhyay, S. Mukherjee, Red edge excitation shift of a deeply embedded membrane probe: implications in water penetration in the bilayer, J. Phys. Chem., B 103 (1999) 8180–8185.
[106] T.X. Xiang, A computer simulation of free-volume distributions and related structural properties in a model lipid bilayer, Biophys. J. 65 (1993) 1108–1120.
[107] S. König, T.M. Bayerl, G. Goddens, D. Richter, E. Sackmann, Hydration dependence of chain dynamics and local diffusion in L-α-dipalmitoylphosphatidylcholine multilayers studied by incoherent quasi-elastic neutron scattering, Biophys. J. 68 (1995) 1871–1880.
[108] S. Paula, A.G. Volkov, A.N.V. Hoek, T.H. Haines, D.W. Deamer, Permeation of protons, potassium ions, and small polar molecules through phospholipid bilayers as a function of membrane thickness, Biophys. J. 70 (1996) 339–348.
[109] A. Finkelstein, Water movement through lipid bilayers, pores and plasma membranes, in: Theory and Reality. Distinguished Lecture Series of the Society of General Physiologists, vol. 4, John Wiley, 1988, pp. 1–228.
[110] M. Jansen, A. Blume, A comparative study of diffusive and osmotic water permeation across bilayers composed of phospholipids with different head groups and fatty acyl chains, Biophys. J. 68 (1995) 997–1008.
[111] H.J. Galla, W. Hartmann, U. Theilen, E. Sackmann, On two-dimensional passive random walk in lipid bilayers and fluid pathways in biomembranes, J. Membr. Biol. 48 (1979) 215–236.
[112] S.J. Marrink, R.M. Sok, H.J.C. Berendsen, Free volume properties of a simulated membrane, J. Chem. Phys. 104 (1996) 9090–9099.
[113] G. Hummer, J.C. Rasalah, J.P. Noworyta, Water conduction through the hydrophobic channel of a carbon nanotube, Nature 414 (2001) 188–190.
[114] T.X. Xiang, B.D. Anderson, Permeability of acetic acid across gel and liquid-crystalline lipid bilayers conforms to free-surface-area theory, Biophys. J. 72 (1997) 223–237.
[115] K. Olbrich, W. Rawicz, D. Needham, E. Evans, Water permeability and mechanical strength of polyunsaturated lipid bilayers, Biophys. J. 79 (2000) 321–327.
[116] P. Laggner, M. Kriechbaum, Phospholipid phase transitions: kinetics and structural mechanism, Chem. Phys. Lipids 57 (1991) 121–145.
[117] J.M. Seddon, G. Cevc, Lipid Polymorphism: Structure and Stability of Lyotropic Mesophases of Phospholipids, in: G. Cevc (Ed.), Posopholipids Handbook, Marcel Dekker, Inc, 1993, pp. 403–454.
[118] R. Koynova, M. Caffrey, Phases and phase transitions of the hydrated phosphatidylethanolamines, Chem. Phys. Lipids 69 (1994) 1–34.
[119] R. Koynova, M. Caffrey, Phases and phase transitions of phosphatidylcholines, Biochim. Biophys. Acta 1376 (1998) 91–145.
[120] H. Binder, W. Pohle, Structural aspects of lyotropic solvation-induced transition in PC and PE assemblies revealed by IR, J. Phys. Chem., B 104 (2000) 12039–12048.
[121] F.H. Johnson, H. Eyring, B.J. Stover, The Theory of Rate Processes in Biology and Medicine, Wiley Interscience, 1974.
[122] P. Grabitz, V.P. Ivanova, T. Heimburg, Relaxation kinetics of lipid membranes and its relation to the heat capacity, Biophys. J. 82 (2002) 299–309.
[123] G. Pabst, H.A.M. Rappolt, S. Bernstorff, P. Laggner, X-ray kinematography of temperature-jump relaxation probes the elastic properties of fluid bilayers, Langmuir 16 (2000) 8994–9001.
[124] B.A. Cunningham, W. Bras, L.J. Lis, P.J. Quinn, Synchrotron X-ray studies of lipids and membranes: a critique, J. Biochem. Biophys. Methods 29 (1994) 87–111.
[125] M. Kodama, M. Kuwabara, S. Seki, Successive phase transition phenomena and phase diagram of the phosphatidylcholine–water systems as revealed by differential scanning calorimetry, Biochim. Biophys. Acta, (1982) 567–570.
[126] S.A. Simon, C.A. Fink, A.K. Kenworthy, T.J. McIntosh, The hydration pressure between lipid bilayers. Comparison of measurements using RX diffraction and calorimetry, Biophys. J. 59 (1991) 538–546.
[127] G. Cevc, D. Marsh, Hydration of non-charged lipid bilayer membranes. Theory and experiments with phosphatidylethanolamine, Biophys. J. 47 (1985) 21–32.
[128] M. Kodama, H. Aoki, H. Takahashi, I. Hatta, Interlamellar waters in dimyristoylphosphatidylethanolamine–water system as studied by calorimetry and X-ray diffraction, Biochim. Biophys. Acta 1329 (1997) 61–73.
[129] T. Heimburg, A model for the lipid pretransition: coupling of ripple formation with the chain-melting transition, Biophys. J. 78 (2000) 1154–1165.
[130] A. Jutila, P.K.J. Kinnunen, Novel features of the main transition of dimyristoylphosphatidylcholine bilayers revealed by fluorescence spectroscopy, J. Phys. Chem., B 101 (1997) 7635–7640.
[131] A.J. Metso, A. Jutila, J.P. Mattila, J.M. Holopainen, P.K.J. Kinnunen, Nature of the main transition of DPPC bilayers inferred from fluorescence spectroscopy, J. Phys. Chem., B 107 (2003) 1251–1257.
[132] M. Rappolt, G. Pabst, G. Rapp, M. Kriechbaum, H. Amenitsch, C. Krenn, S. Bernstorff, P. Laggner, New evidence for gel–liquid crystalline phase coexistence in the ripple phase of phosphatidylcholines, Eur. Biophys. J. 29 (2000) 125–133.
[133] K. Pressl, K. Jorgensen, P. Laggner, Characterization of the submain-transition in distearoylphosphatidylcholine studied by simultaneous small- and wide-angle X-ray diffraction, Biochim. Biophys. Acta 1325 (1997) 1–7.
[134] C. Trandum, P. Westh, K. Jorgensen, Slow relaxation of the submain transition in multilamellar phosphatidylcholine vesicles, Biochim. Biophys. Acta 1421 (1999) 207–212.
[135] J.F. Nagle, H.I. Petrache, N. Gouliev, S. Tristram-Nagle, Y. Lin, R.M. Suter, K. Gawrisch, Phys. Rev., E 58 (1998) 7769.
[136] G. Pabst, J. Katsaras, V.A. Raghunathan, M. Rappolt, Structure and interactions in the anomalous swelling regime of phospholipid bilayers, Langmuir 19 (2003) 1716–1722.
[137] L. Terminassian-Saraga, G. Madelmont, Subtransition and hydration studies of fully hydrated DPPC gel phase, J. Colloid Interface Sci. 99 (1984) 420–426.
[138] J.M. Seddon, Structure of the inverted hexagonal (H_{II})phase nonlamellar transitions of lipids, Biochim. Biophys. Acta 1031 (1990) 1–69.
[139] W. Helfrich, Elastic properties of lipid bilayers: theory and possible experiments, Z. Naturforsch. 28C (1973) 693–703.
[140] M.M. Kozlov, S. Leikin, R.P. Rand, Bending, hydration and interstitial energies quantitatively account for the hexagonal-lamellar-hexagonal reentrant phase transition in dioleoylphosphatidylethanolamine, Biophys. J. 67 (1994) 1603–1611.
[141] G.S. Toombes, A.C. Finnefrock, M.W. Tate, S.M. Gruner, Determination of L_{α}-H_{II} phase transition temperature for 1, 2-dioleoyl-*sn*-glycero-3-phosphatidylethanolamine, Biophys. J. 82 (2002) 2504–2510.
[142] J. Katsaras, K.R. Jeffrey, D.S.C. Yang, R.M. Epand, Direct evidence for the partial dehydration of phosphatidylethanolamine bilayers on approaching the hexagonal phase, Biochem. 32 (1993) 10700–10707.
[143] P.E. Harper, D.A. Mannock, R.N.A.H. Lewis, R.N. McElhaney, S. Gruner, X-ray diffraction of some phosphatidylethanolamine lamellar and inverted hexagonal phases, Biophys. J. 81 (2001) 2693–2706.
[144] H. Binder, T. Gutberlet, A. Anikin, G. Klose, Hydration of the dienic lipid dioctadecadienoyl PC in the lamellar phase. An IR linear dichroism and XR study on headgroup orientation, water ordering and bilayer dimensions, Biophys. J. 74 (1998) 1908–1923.

[145] H. Binder, A. Anikin, B. Kohlstrunk, G. Klose, Hydration-induced gel states of the dienic lipid 1, 2-bis (2, 4 octadecadienoyl)-*sn*-glycero 3-phosphorylcholine and their characterization using IR spectroscopy, J. Phys. Chem., B 101 (1997) 6618–6628.
[146] B. Bechinger, J. Seelig, Conformational changes of the phosphatidylcholine headgroup due to membrane dehydration. A ^{2}H-NMR study, Chem. Phys. Lipids 58 (1991) 1–5.
[147] H. Binder, B. Kohlstrunk, W. Pohle, Thermodynamical and kinetic aspects of lyotropic solvation-induced transition in PC and PE assemblies revealed by humidity titration calorimetry, J. Phys. Chem., B 104 (2000) 12049–12055.
[148] W. Blokzijl, J.B.F.N. Engberts, Hydrophobic effects. Opinions and facts, Angew. Chem. Int. Ed. Engl. 32 (1993) 1545–1579.
[149] S. Kint, P.H. Wermer, J.R. Scherer, Raman spectra of hydrated phospholipid bilayers: 2. Water and head-group interactions, J. Phys. Chem. 96 (1992) 446–452.
[150] W.C. Hung, F.Y. Chen, H.W. Huang, Order–disorder transition in bilayers of diphytanoyl phosphatidylcholine, Biochim. Biophys. Acta 1467 (2000) 198–206.
[151] W. Pohle, C. Selle, D.R. Gauger, K. Brandenburg, Lyotropic phase transitions in phospholipids as evidenced by small-angle synchrotron X-ray scattering, J. Biomol. Struct. Dyn. 19 (2001) 351–364.
[152] A. Enders, G. Nimtz, Dielectric relaxation study of dynamic properties of hydrated phospholipid bilayers, Ber. Bunsenges. Phys. Chem. 88 (1984) 512–517.
[153] V.A. Parsegian, R.P. Rand, D.C. Rau, Osmotic stress, crowding, preferential hydration, and binding: a comparison of perspectives, Proc. Natl. Acad. Sci. 97 (2000) 3987–3992.
[154] P. Mentré, L'eau dans la cellule. Une interface hétérogène et dynamique des macromolécules, 1st ed., Masson, Paris, 1995.
[155] R.P. Rand, Raising water to new heights, Science 256 (1992) 618.
[156] J.F. Nagle, R. Zhang, S. Tristram-Nagle, W.J. Sun, H.I. Petrache, R.M. Suter, X-ray structure determination of fully hydrated Lα phase DPPC bilayers, Biophys. J. 70 (1996) 1419–1431.